CHAPTER 9

# Direct detection receiver performance considerations

## 9.1 Introduction

The receiver in an intensity-modulated/direct detection (IM/DD) optical fiber communication system (see Section 7.5) essentially consists of the photodetector plus an amplifier with possibly additional signal processing circuits. Therefore the receiver initially converts the optical signal incident on the detector into an electrical signal, which is then amplified before further processing to extract the information originally carried by the optical signal.

The importance of the detector in the overall system performance was stressed in Chapter 8. However, it is necessary to consider the properties of this device in the context of the associated circuitry combined in the receiver. It is essential that the detector performs efficiently with the following amplifying and signal processing circuits. Inherent to this process is the separation of the information originally contained in the optical signal from the noise generated within the rest of the system and in the receiver itself, as well as any limitations on the detector response imposed by the associated circuits. These factors play a crucial role in determining the performance of the system.

In order to consider receiver design it is useful to regard the limit on the performance of the system set by the signal-to-noise ratio (SNR) at the receiver. It is therefore necessary to outline noise sources within optical fiber systems. The noise in these systems has different origins from that of copper-based systems. Both types of system have thermal noise generated in the receiver. However, although optical fiber systems exhibit little crosstalk the noise generated within the detector must be considered, as well as the noise properties associated with the electromagnetic carrier.

In Section 9.2 we therefore briefly review the major noise mechanisms which are present in direct detection optical fiber communication receivers prior to more detailed discussion of the limitations imposed by photon (or quantum) noise in both digital and analog transmission. This is followed in Section 9.3 with a more specific discussion of the noise associated with the two major receiver types (i.e. employing *p–i–n* and avalanche photodiode detectors). Expressions for the SNRs of these two receiver types are also developed in this section. Section 9.4 considers the noise and bandwidth performance of common preamplifier structures utilized in the design of optical fiber receivers. In Section 9.5 we present a brief account of low-noise field effect transistor (FET) preamplifiers which find wide use within optical fiber communication receivers. This discussion also includes consideration of *p–i–n* photodiode/FET (PIN–FET) hybrid receiver circuits which have been developed for optical fiber communications. Finally, major high-performance receiver design strategies to provide low-noise and high-bandwidth operation as well as wide dynamic range are described in Section 9.6.

## 9.2 Noise

Noise is a term generally used to refer to any spurious or undesired disturbances that mask the received signal in a communication system. In optical fiber communication systems we are generally concerned with noise due to spontaneous fluctuations rather than erratic disturbances which may be a feature of copper-based systems (due to electromagnetic interference etc.).

There are three main types of noise due to spontaneous fluctuations in optical fiber communication systems: thermal noise, dark current noise and quantum noise.

### 9.2.1 Thermal noise

This is the spontaneous fluctuation due to thermal interaction between, say, the free electrons and the vibrating ions in a conducting medium, and it is especially prevalent in resistors at room temperature.

The thermal noise current $i_t$ in a resistor $R$ may be expressed by its mean square value [Ref. 1] and is given by:

$$\overline{i_t^2} = \frac{4KTB}{R} \tag{9.1}$$

where $K$ is Boltzmann's constant, $T$ is the absolute temperature and $B$ is the post-detection (electrical) bandwidth of the system (assuming the resistor is in the optical receiver).

## 9.2.2 Dark current noise

When there is no optical power incident on the photodetector a small reverse leakage current still flows from the device terminals. This dark current (see Section 8.4.2) contributes to the total system noise and gives random fluctuations about the average particle flow of the photocurrent. It therefore manifests itself as shot noise [Ref. 1] on the photocurrent. Thus the dark current noise $\overline{i_d^2}$ is given by:

$$\overline{i_d^2} = 2eBI_d \tag{9.2}$$

where $e$ is the charge on an electron and $I_d$ is the dark current. It may be reduced by careful design and fabrication of the detector.

## 9.2.3 Quantum noise

The quantum nature of light was discussed in Section 6.2.1 and the equation for the energy of this quantum or photon was stated as $E = hf$. The quantum behavior of electromagnetic radiation must be taken into account at optical frequencies since $hf > KT$ and quantum fluctuations dominate over thermal fluctuations.

The detection of light by a photodiode is a discrete process since the creation of an electron–hole pair results from the absorption of a photon, and the signal emerging from the detector is dictated by the statistics of photon arrivals. Hence the statistics for monochromatic coherent radiation arriving at a detector follow a discrete probability distribution which is independent of the number of photons previously detected.

It is found that the probability $P(z)$ of detecting $z$ photons in time period $\tau$ when it is expected on average to detect $z_m$ photons obeys the Poisson distribution [Ref. 2]:

$$P(z) = \frac{z_m^z \exp(-z_m)}{z!} \tag{9.3}$$

where $z_m$ is equal to the variance of the probability distribution. This equality of the mean and the variance is typical of the Poisson distribution. From Eq. (8.7) the electron rate $r_e$ generated by incident photons is $r_e = \eta P_o / hf$. The number of electrons generated in time $\tau$ is equal to the average number of photons detected over this time period $z_m$. Therefore:

$$z_m = \frac{\eta P_o \tau}{hf} \tag{9.4}$$

The Poisson distributions for $z_m = 10$ and $z_m = 1000$ are illustrated in Figure 9.1 and represent the detection process for monochromatic coherent light.

Incoherent light is emitted by independent atoms and therefore there is no phase relationship between the emitted photons. This property dictates an exponential intensity distribution for incoherent light which if averaged over the Poisson distribution [Ref. 2] gives:

$$P(z) = \frac{z_m^z}{(1 + z_m)^{z+1}} \tag{9.5}$$

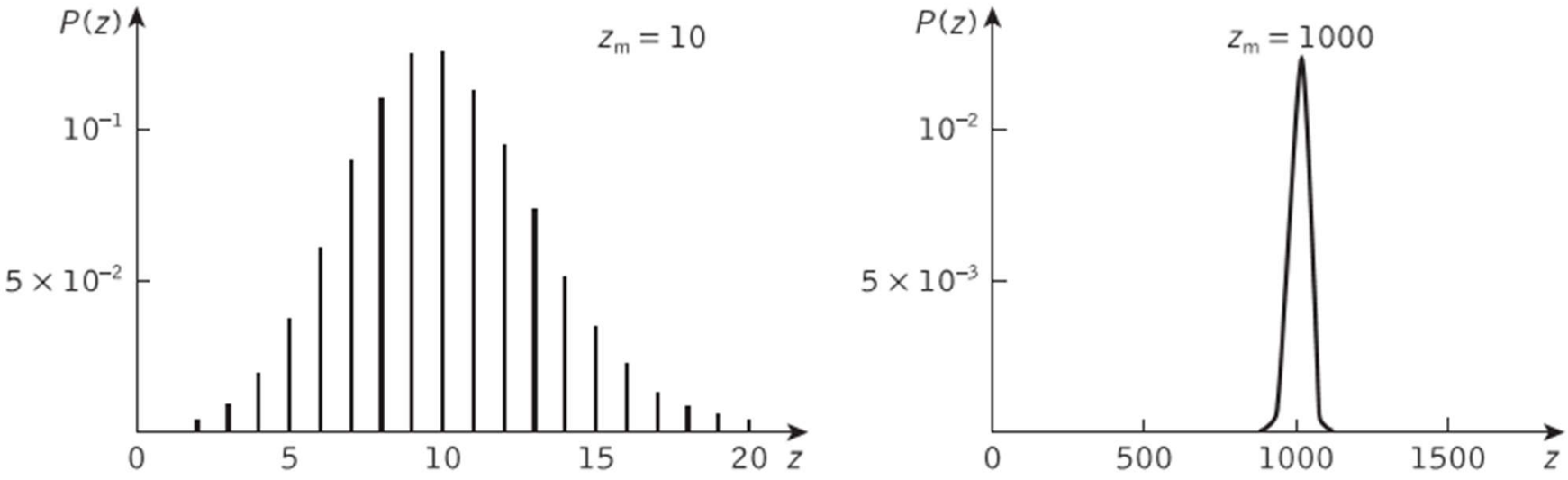


**Figure 9.1** Poisson distributions for $z_m = 10$ and $z_m = 1000$

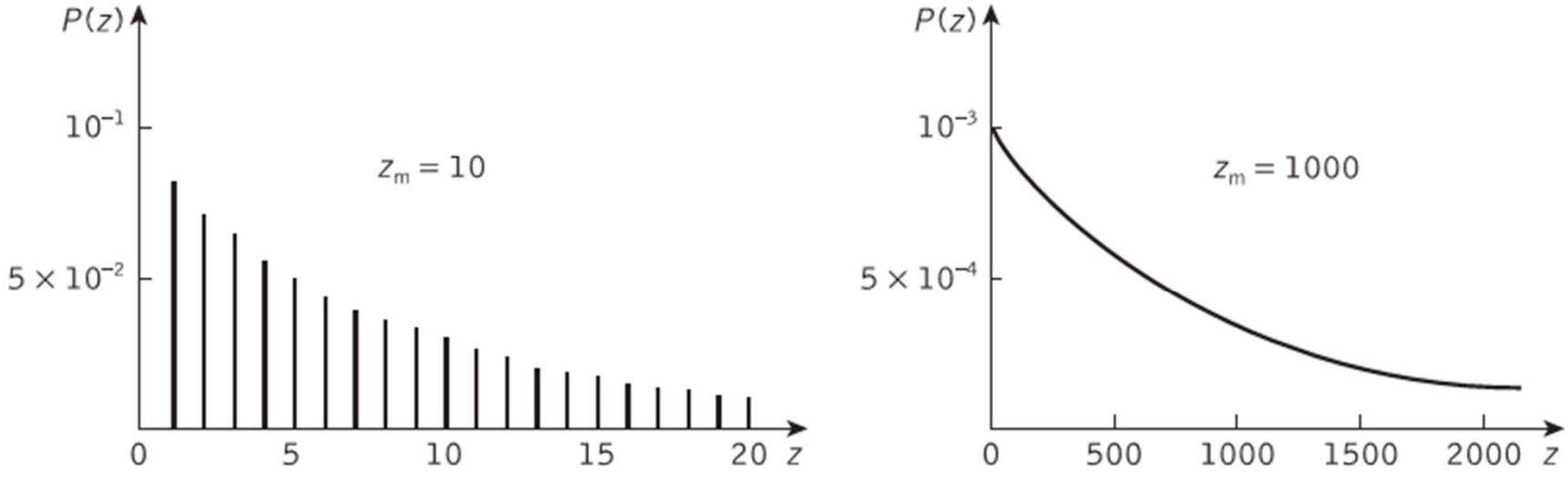


**Figure 9.2** Probability distributions indicating the statistical fluctuations of incoherent light for $z_m = 10$ and $z_m = 1000$

Equation (9.5) is identical to the Bose–Einstein distribution [Ref. 3] which is used to describe the random statistics of light emitted in black body radiation (thermal light). The statistical fluctuations for incoherent light are illustrated by the probability distributions shown in Figure 9.2.

## 9.2.4 Digital signaling quantum noise

For digital optical fiber systems it is possible to calculate a fundamental lower limit to the energy that a pulse of light must contain in order to be detected with a given probability of error. The premise on which this analysis is based is that the ideal receiver has a sufficiently low amplifier noise to detect the displacement current of a single electron–hole pair generated within the detector (i.e. an individual photon may be detected). Thus in the absence of light, and neglecting dark current, no current will flow. Therefore the only way an error can occur is if a light pulse is present and no electron–hole pairs are generated. The probability of no pairs being generated when a light pulse is present may be obtained from Eq. (9.3) and is given by:

$$P(0|1) = \exp(-z_m) \tag{9.6}$$

Thus in the receiver described $P(0|1)$ represents the system error probability $P(e)$ and therefore:

$$P(\mathrm{e}) = \exp(-z_{\mathrm{m}}) \tag{9.7}$$

However, it must be noted that the above analysis assumes that the photodetector emits no electron–hole pairs in the absence of illumination. In this sense it is considered perfect. Equation (9.7) therefore represents an absolute receiver sensitivity and allows the determination of a fundamental limit in digital optical communications. This is the minimum pulse energy $E_{\mathrm{min}}$ required to maintain a given bit-error-rate (BER) which any practical receiver must satisfy and is known as the quantum limit.

## Example 9.1

A digital optical fiber communication system operating at a wavelength of 1 μm requires a maximum bit-error-rate of $10^{-9}$. Determine:

(a) the theoretical quantum limit at the receiver in terms of the quantum efficiency of the detector and the energy of an incident photon;

(b) the minimum incident optical power required at the detector in order to achieve the above bit-error-rate when the system is employing ideal binary signaling at 10 Mbit $s^{-1}$, and assuming the detector is ideal.

*Solution:* (a) From Eq. (9.7) the probability of error:

$$P(\mathrm{e}) = \exp(-z_\mathrm{m}) = 10^{-9}$$

and thus $z_\mathrm{m} = 20.7$.

$z_\mathrm{m}$ corresponds to an average number of photons detected in a time period $\tau$ for a BER of $10^{-9}$.

From Eq. (9.4):

$$z_\mathrm{m} = \frac{\eta P_\mathrm{o} \tau}{hf} = 20.7$$

Hence the minimum pulse energy or quantum limit:

$$E_{\min} = P_o \tau = \frac{20.7hf}{\eta}$$

Thus the quantum limit at the receiver to maintain a maximum BER of $10^{-9}$ is:

$$\frac{20.7hf}{\eta}$$

(b) From part (a) the minimum pulse energy:

$$P_o \tau = \frac{20.7hf}{\eta}$$

Therefore the average received optical power required to provide the minimum pulse energy is:

$$P_o = \frac{20.7hf}{\tau\eta}$$

However, for ideal binary signaling there are an equal number of ones and zeros (50% in the on state and 50% in the off state). Thus the average received optical power may be considered to arrive over two bit periods, and:

$$P_o(\text{binary}) = \frac{20.7hf}{2\tau\eta} = \frac{20.7hfB_T}{2\eta}$$

where $B_T$ is the bit rate. At a wavelength of 1 μm, $f = 2.998 \times 10^{14}$ Hz, and assuming an ideal detector, $\eta = 1$.

Hence:

$$P_o(\text{binary}) = \frac{20.7 \times 6.626 \times 10^{-34} \times 2.998 \times 10^{14} \times 10^7}{2}$$

$$= 20.6 \text{ pW}$$

In decibels (dB):

$$P_o \text{ in dB} = 10 \log_{10} \frac{P_o}{P_r}$$

where $P_r$ is a reference power level.

When the reference power level is 1 watt:

$$\begin{aligned} P_o &= 10 \log_{10} P_o \quad \text{where } P_o \text{ is expressed in watts} \\ &= 10 \log_{10} 2.06 \times 10^{-11} \\ &= 3.14 - 110 \\ &= -106.9 \text{ dBW} \end{aligned}$$

When the reference power level is 1 milliwatt:

$$\begin{aligned} P_o &= 10 \log_{10} 2.06 \times 10^{-8} \\ &= 3.14 - 80 \\ &= -76.9 \text{ dBm} \end{aligned}$$

Therefore the minimum incident optical power required at the receiver to achieve an error rate of $10^{-9}$ with ideal binary signaling is 20.6 pW or –76.9 dBm.

The result of Example 9.1 is a theoretical limit and in practice receivers are generally found to be at least 10 dB less sensitive. Furthermore, although some 20.7 photons are required in order to detect a binary 1 with a BER of $10^{-9}$, it is clear that these photons can arrive at the receiver over two bit periods if an equal number of transmitted ones and zeros are assumed (i.e. there are no photons transmitted in the zero-bit periods). Hence the 20.7 photons per pulse requirement can be considered as an average of around 10.4 photons per bit at the quantum limit.

## 9.2.5 Analog transmission quantum noise

In analog optical fiber systems quantum noise manifests itself as shot noise which also has Poisson statistics [Ref. 1]. The shot noise current $i_s$ on the photocurrent $I_p$ is given by:

$$\overline{i_s^2} = 2eBI_p \tag{9.8}$$

Neglecting other sources of noise the SNR at the receiver may be written as:

$$\frac{S}{N} = \frac{I_p^2}{i_s^2} \tag{9.9}$$

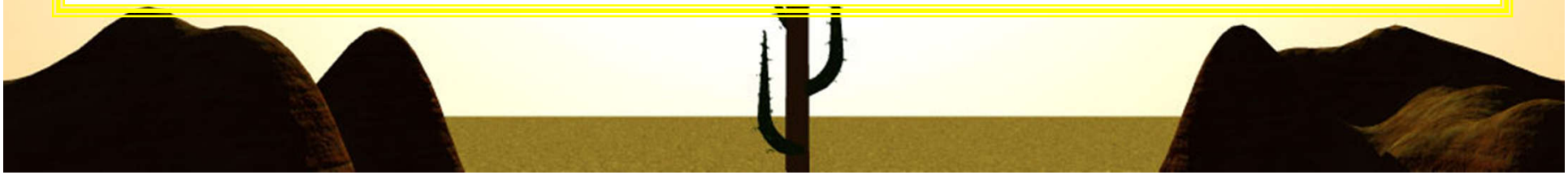

Substituting for $\overline{i_s^2}$ from Eq. (9.8) gives:

$$\frac{S}{N} = \frac{I_p}{2eB} \tag{9.10}$$

The expression for the photocurrent $I_p$ given in Eq. (8.8) allows the SNR to be obtained in terms of the incident optical power $P_o$:

$$\frac{S}{N} = \frac{\eta P_o e}{hf 2eB} = \frac{\eta P_o}{2hfB} \tag{9.11}$$

Equation (9.11) allows calculation of the incident optical power required at the receiver in order to obtain a specified SNR when considering quantum noise in analog optical fiber systems.

## Example 9.2

An analog optical fiber system operating at a wavelength of 1 μm has a post-detection bandwidth of 5 MHz. Assuming an ideal detector and considering only quantum noise on the signal, calculate the incident optical power necessary to achieve an SNR of 50 dB at the receiver.

*Solution:* From Eq. (9.11), the SNR is:

$$\frac{S}{N} = \frac{\eta P_o}{2hfB}$$

Hence:

$$P_o = \left(\frac{S}{N}\right)\frac{2hfB}{\eta}$$

For $S/N = 50$ dB, when considering signal and noise powers:

$$10 \log_{10} \frac{S}{N} = 50$$

and therefore $S/N = 10^5$

At 1 μm, $f = 2.998 \times 10^{14}$ Hz. For an ideal detector $\eta = 1$ and thus the incident optical power:

$$P_o = \frac{10^5 \times 2 \times 6.626 \times 10^{-34} \times 2.998 \times 10^{14} \times 5 \times 10^6}{1}$$

$$= 198.6 \text{ nW}$$

In dBm:

$$P_o = 10 \log_{10} 198.6 \times 10^{-6}$$
$$= -40 + 2.98$$
$$= -37.0 \text{ dBm}$$

Therefore the incident optical power required to achieve an SNR of 50 dB at the receiver is 198.6 nW which is equivalent to −37.0 dBm.

In practice, receivers are less sensitive than Example 9.2 suggests and thus in terms of the absolute optical power requirements analog transmission compares unfavorably with digital signaling.

However, it should be noted that there is a substantial difference in information transmission capacity between the digital and analog cases (over similar bandwidths) considered in Examples 9.1 and 9.2. For example, a 10 Mbit $s^{-1}$ digital optical fiber communication system would provide only about 150 speech channels using standard baseband digital transmission techniques (see Section 12.5). In contrast a 5 MHz analog system, again operating in the baseband, could provide as many as 1250 similar bandwidth ($\simeq$3.4 kHz) speech channels. A comparison of signal to quantum noise ratios between the two transmission methods, taking account of this information capacity aspect, yields less disparity although digital signaling still proves far superior. For instance, applying the figures quoted above within Examples 9.1 and 9.2, in order to compare two systems capable of transmitting the same number of speech channels (e.g. digital bandwidth of 10 Mbit $s^{-1}$ and analog bandwidth of 600 kHz), gives a difference in absolute sensitivity in favor of digital transmission of approximately 31 dB. This indicates a reduction of around 9 dB on the 40 dB difference obtained by simply comparing the results over similar bandwidths. Nevertheless, it is clear that digital signaling techniques still provide a significant benefit in relation to quantum noise when employed within optical fiber communications.

## 9.3 Receiver noise

In order to investigate the optical receiver in greater detail it is necessary to consider the relative importance and interplay of the various types of noise mentioned in the preceding section. This is dependent on both the method of demodulation and the type of device used for detection.

The conditions for coherent detection are not met in IM/DD optical fiber systems for the reasons outlined in Section 7.5. Thus heterodyne and homodyne detection, which are very sensitive techniques and provide excellent rejection of adjacent channels, are not used, as the optical signal arriving at the receiver tends to be incoherent. In practice the vast majority of installed optical fiber communication systems use incoherent or direct detection in which the variation of the optical power level is monitored and no information is carried in the phase or frequency content of the signal. Therefore, the noise considerations in this section are based on a receiver employing direct detection of the modulated optical carrier which gives the same SNR as an unmodulated optical carrier. The significant developments in coherent optical fiber transmission, however, which have taken place over recent years are described in Chapter 13. Nevertheless, the major performance parameters associated with direct detection receivers which are discussed in this section and the following ones also apply to coherent optical receivers.

Figure 9.3 shows a block schematic of the front end of an optical receiver and the various noise sources associated with it. The majority of the noise sources shown apply to both

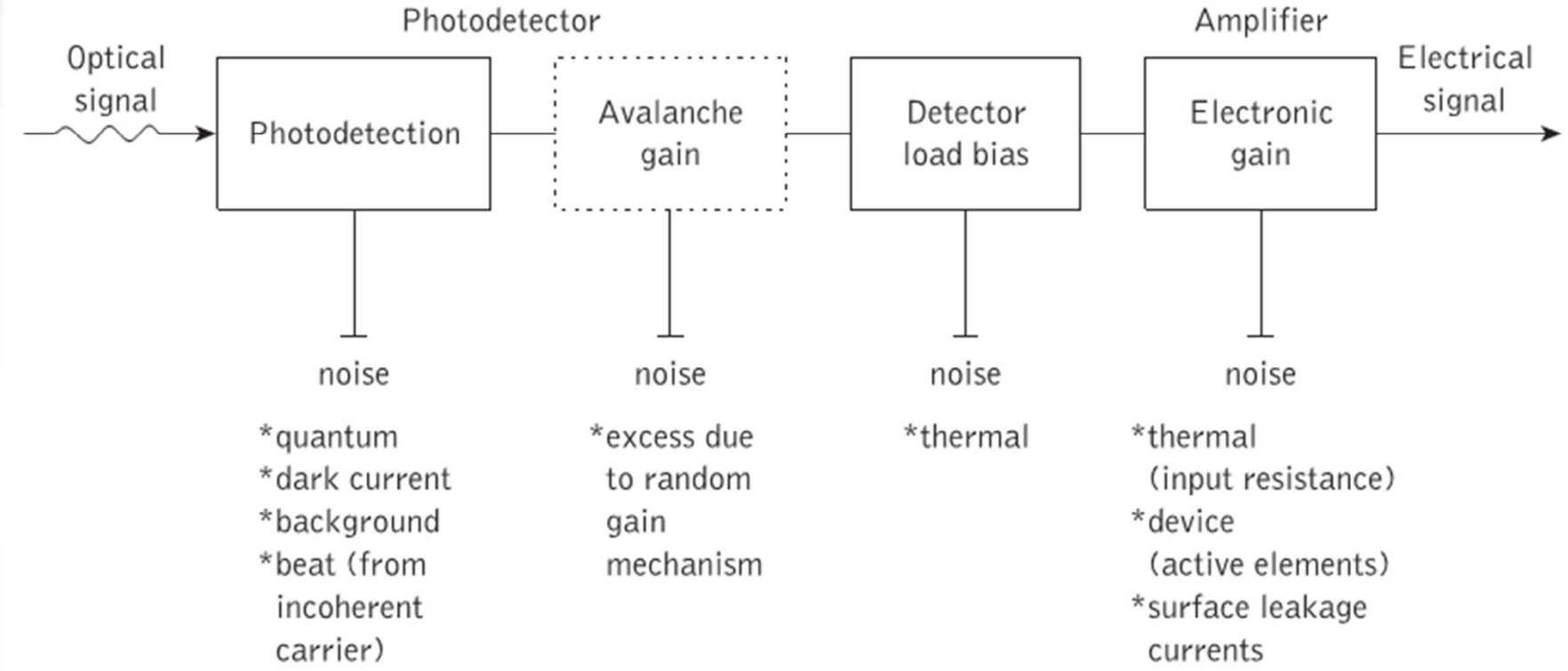


**Figure 9.3** Block schematic of the front end of an optical receiver showing the various sources of noise

main types of optical detector (*p–i–n* and avalanche photodiode). The noise generated from background radiation, which is important in atmospheric propagation and some copper-based systems, is negligible in both types of optical fiber receiver, and thus is often ignored. Also the beat noise generated from the various spectral components of the incoherent optical carrier can be shown to be insignificant [Ref. 4] with multimode propagation and hence will not be considered. It is necessary, however, to take into account the other sources of noise shown in Figure 9.3.

The avalanche photodiode receiver is the most complex case as it includes noise resulting from the random nature of the internal gain mechanism (dotted in Figure 9.3). It is therefore useful to consider noise in optical fiber receivers employing photodiodes without internal gain, before avalanche photodiode receivers are discussed.

## 9.3.1 The *p–n* and *p–i–n* photodiode receiver

The two main sources of noise in photodiodes without internal gain are dark current noise and quantum noise, both of which may be regarded as shot noise on the photocurrent (i.e. effectively, analog quantum noise). When the expressions for these noise sources given in Eqs (9.2) and (9.4) are combined the total shot noise $\overline{i_{TS}^2}$ is given by:

$$\overline{i_{TS}^2} = 2eB(I_p + I_d) \tag{9.12}$$

If it is necessary to take the noise due to the background radiation into account then the expression given in Eq. (9.12) may be expanded to include the background-radiation-induced photocurrent $I_b$ giving:

$$\overline{i_{TS}^2} = 2eB(I_p + I_d + I_b) \tag{9.13}$$

However, as $I_b$ is usually negligible the expression given in Eq. (9.12) will be used in the further analysis.

When the photodiode is without internal avalanche gain, thermal noise from the detector load resistor and from active elements in the amplifier tends to dominate. This is especially the case for wideband systems operating in the 0.8 to 0.9 μm wavelength band because the dark currents in well-designed silicon photodiodes can be made very small. The thermal noise $\overline{i_t^2}$ due to the load resistance $R_L$ may be obtained from Eq. (9. 1) and is given by:

$$\overline{i_t^2} = \frac{4KTB}{R_L} \tag{9.14}$$

The dominating effect of this thermal noise over the shot noise in photodiodes without internal gain may be observed in Example 9.3.

Example 9.3 does not include the noise sources within the amplifier, shown in Figure 9.3. These noise sources, associated with both the active and passive elements of the amplifier, can be represented by a series voltage noise source $\overline{v_a^2}$ and a shunt current noise source $\overline{i_a^2}$.

## Example 9.3

A silicon *p–i–n* photodiode incorporated into an optical receiver has a quantum efficiency of 60% when operating at a wavelength of 0.9 μm. The dark current in the device at this operating point is 3 nA and the load resistance is 4 kΩ.

The incident optical power at this wavelength is 200 nW and the post-detection bandwidth of the receiver is 5 MHz. Compare the shot noise generated in the photodiode with the thermal noise in the load resistor at a temperature of 20 °C.

*Solution:* From Eq. (8.8) the photocurrent is given by:

$$I_p = \frac{\eta P_o e}{hf} = \frac{\eta P_o e \lambda}{hc}$$

Therefore:

$$I_p = \frac{0.6 \times 200 \times 10^{-9} \times 1.602 \times 10^{-19} \times 0.9 \times 10^{-6}}{6.626 \times 10^{-34} \times 2.998 \times 10^{8}}$$

$$= 87.1 \text{ nA}$$

From Eq. (9.12) the total shot noise is:

$$\overline{i_{TS}^2} = 2eB(I_d + I_p)$$
$$= 2 \times 1.602 \times 10^{-19} \times 5 \times 10^{6} \left[(3 + 87.1) \times 10^{-9}\right]$$
$$= 1.44 \times 10^{-19} \text{ A}^2$$

and the root mean square (rms) shot noise current is:

$$(\overline{i_{TS}^2})^{\frac{1}{2}} = 3.79 \times 10^{-10}\ \text{A}$$

The thermal noise in the load resistor is given by Eq. (9.14):

$$\overline{i_t^2} = \frac{4KTB}{R_L}$$

$$= \frac{4 \times 1.381 \times 10^{-23} \times 293 \times 5 \times 10^6}{4 \times 10^3}$$

$$= 2.02 \times 10^{-17}\ \text{A}^2$$

($T = 20\ ^\circ\text{C} = 293\ \text{K}$).

Therefore the rms thermal noise current is:

$$(\overline{i_t^2})^{\frac{1}{2}} = 4.49 \times 10^{-9}\ \text{A}$$

In this example the rms thermal noise current is a factor of 12 greater than the total rms shot noise current.

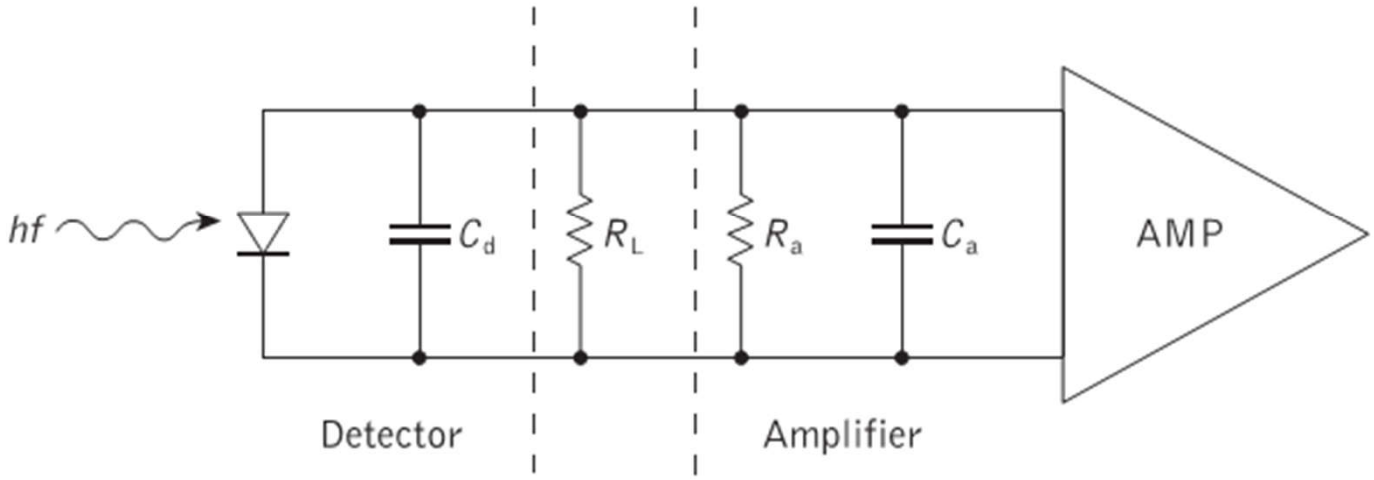


**Figure 9.4** The equivalent circuit for the front end of an optical fiber receiver

Thus the total noise associated with the amplifier $\overline{i_{amp}^2}$ is given by:

$$\overline{i_{amp}^2} = \int_0^B (\overline{i_a^2} \times \overline{v_a^2} \mid Y \mid^2)\, \mathrm{d}f \tag{9.15}$$

where $Y$ is the shunt admittance (combines the shunt capacitances and resistances) and $f$ is the frequency. An equivalent circuit for the front end of the receiver, including the effective input capacitance $C_a$ and resistance $R_a$ of the amplifier, is shown in Figure 9.4. The capacitance of the detector $C_d$ is also shown and the noise resulting from $C_d$ is usually included in the expression for $\overline{i_{amp}^2}$ given in Eq. (9.15).

The SNR for the $p$–$n$ or $p$–$i$–$n$ photodiode receiver may be obtained by summing the noise contributions from Eqs (9.12), (9.14) and (9.15). It is given by:

$$\frac{S}{N} = \frac{I_p^2}{2eB(I_p + I_d) + \dfrac{4KTB}{R_L} + \overline{i_{amp}^2}} \tag{9.16}$$

The thermal noise contribution may be reduced by increasing the value of the load resistor $R_L$, although this reduction may be limited by bandwidth considerations which are discussed later. Also, the noise associated with the amplifier $\overline{i_{amp}^2}$ may be reduced with low detector and amplifier capacitance.

However, when the noise associated with the amplifier $\overline{i_{amp}^2}$ is referred to the load resistor $R_L$, the noise figure $F_n$ [Ref. 1] for the amplifier may be obtained. This allows $\overline{i_{amp}^2}$ to be combined with the thermal noise from the load resistor $\overline{i_t^2}$ to give:

$$\overline{i_t^2} \times \overline{i_{amp}^2} = \frac{4KTBF_n}{R_L} \tag{9.17}$$

The expression for the SNR given in Eq. (9.16) can now be written in the form:

$$\frac{S}{N} = \frac{I_p^2}{2eB(I_p + I_d) + \dfrac{4KTBF_n}{R_L}} \tag{9.18}$$

Thus if the noise figure $F_n$ for the amplifier is known, Eq. (9.18) allows the SNR to be determined.

## Example 9.4

The receiver in Example 9.3 has an amplifier with a noise figure of 3 dB. Determine the SNR at the output of the receiver under the same conditions as Example 9.3.

*Solution:* From Example 9.3:

$$I_p = 87.1 \times 10^{-9}\ \text{A}$$
$$\overline{i_{TS}^2} = 1.44 \times 10^{-19}\ \text{A}^2$$
$$\overline{i_t^2} = 2.02 \times 10^{-17}\ \text{A}^2$$

The amplifier noise figure:

$$F_n = 3\ \text{dB}$$
$$= 10 \log_{10} 2$$

Thus $F_n$ may be considered as $\times 2$.

In Eq. (9.18) the SNR is given by:

$$\frac{S}{N} = \frac{I_p^2}{2eB(I_p + I_d) + \frac{4KTBF_n}{R_L}}$$

$$= \frac{I_p^2}{\overline{i_{TS}^2} + (\overline{i_t^2} \times F_n)}$$

$$= \frac{(87.1 \times 10^{-9})^2}{(1.44 \times 10^{-19}) + (2.02 \times 10^{-17} \times 2)}$$

$$= 1.87 \times 10^2$$

SNR in dB = $10 \log_{10} 1.87 \times 10^2 = 22.72$ dB.

Alternatively it is possible to conduct the calculation in dB if we neglect the shot noise (say, $\overline{i_{TS}^2} = 0$).

In dB:

$$I_p = 9.40 - 80 = -70.60$$

Hence:

$$I_p^2 = -141.20 \text{ dB}$$

and:

$$\overline{i_t^2} = 3.05 - 170 = -166.95 \text{ dB}$$

The amplifier noise figure $F_n = 3$ dB.

Therefore:

$$\frac{S}{N} = -141.20 + 166.95 - 3$$

$$= 22.75 \text{ dB}$$

A slight difference in the final answer may be noted. This is due to the neglected shot noise term.

A quantity discussed in Section 8.8.3 which is often used in the specification of optical detectors (or detector–amplifier combinations) is the noise equivalent power (*NEP*). It is defined as the amount of incident optical power $P_o$ per unit bandwidth required to produce an output power equal to the detector (or detector–amplifier combination) output noise power. The *NEP* is therefore the value of $P_o$ which gives an output SNR of unity. Thus the lower the *NEP* for a particular detector (or detector–amplifier combination), the less optical power is needed to obtain a particular SNR.

## 9.3.2 Receiver capacitance and bandwidth

Considering the equivalent circuit shown in Figure 9.4, the total capacitance for the front end of an optical receiver $C_T$ is given by:

$$C_T = C_d + C_a \tag{9.19}$$

where $C_d$ is the detector capacitance and $C_a$ is the amplifier input capacitance. It is important that this total capacitance is minimized not only from the noise considerations discussed previously, but also from the bandwidth penalty which is incurred due to the time constant of $C_T$ and the load resistance $R_L$. We assume here that $R_L$ is the total loading on the detector and therefore have neglected the amplifier input resistance $R_a$. However, in practical receiver configurations $R_a$ may have to be taken into account (see Section 9.4.1). The reciprocal of the time constant $2\pi R_L C_T$ must be greater than, or equal to, the post-detection bandwidth $B$:

$$\frac{1}{2\pi R_L C_T} \geq B \tag{9.20}$$

When the equality exists in Eq. (9.20) it defines the maximum possible value of $B$ for the straightforward termination indicated in Figure 9.4.

Assuming that the total capacitance may be minimized, then the other parameter which affects $B$ is the load resistance $R_L$. To increase $B$ it is necessary to reduce $R_L$. However, this introduces a thermal noise penalty as may be seen from Eq. (9.14) where both the increase in $B$ and decrease in $R_L$ contribute to an increase in the thermal noise. A trade-off therefore

exists between the maximum bandwidth and the level of thermal noise which may be tolerated. This is especially important in receivers which are dominated by thermal noise.

## Example 9.5

A photodiode has a capacitance of 6 pF. Calculate the maximum load resistance which allows an 8 MHz post-detection bandwidth.

Determine the bandwidth penalty with the same load resistance when the following amplifier also has an input capacitance of 6 pF.

*Solution:* From Eq. (9.20) the maximum bandwidth is given by:

$$B = \frac{1}{2\pi R_L C_d}$$

Therefore the maximum load resistance:

$$R_L\ (\text{max}) = \frac{1}{2\pi C_d B} = \frac{1}{2\pi \times 6 \times 10^{-12} \times 8 \times 10^6}$$

$$= 3.32\ \text{k}\Omega$$

Thus for an 8 MHz bandwidth the maximum load resistance is 3.32 kΩ.

Also, considering the amplifier capacitance, the maximum bandwidth:

$$B = \frac{1}{2\pi R_L (C_d + C_a)} = \frac{1}{2\pi \times 3.32 \times 10^3 \times 12 \times 10^{-12}}$$

$$= 4\ \text{MHz}$$

As would be expected, the maximum post-detection bandwidth is halved.

## 9.3.3 Avalanche photodiode (APD) receiver

The internal gain mechanism in an APD increases the signal current into the amplifier and so improves the SNR because the load resistance and amplifier noise remain unaffected (i.e. the thermal noise and amplifier noise figure are unchanged). However, the dark current and quantum noise are increased by the multiplication process and may become a limiting factor. This is because the random gain mechanism introduces excess noise into the receiver in terms of increased shot noise above the level that would result from amplifying only the primary shot noise. Thus if the photocurrent is increased by a factor $M$ (mean avalanche multiplication factor), then the shot noise is also increased by an excess noise factor $M^x$, such that the total shot noise $\overline{i_{SA}^2}$ is now given by:

$$\overline{i_{SA}^2} = 2eB(I_p + I_d)M^{2+x} \tag{9.21}$$

where $x$ is between 0.3 and 0.5 for silicon APDs and between 0.7 and 1.0 for germanium or III–V alloy APDs.

Equation (9.21) is often used as the total shot noise term in order to compute the SNR, although there is a small amount of shot noise current which is not multiplied through impact ionization. The shot noise current in the detector which is not multiplied is a device parameter and may be considered as an extra shot noise term. However, it tends to be insignificant in comparison with the multiplied shot noise and is therefore neglected in the further analysis (i.e. all shot noise is assumed to be multiplied).

The SNR for the APD may be obtained by summing the combined noise contribution from the load resistor and the amplifier given in Eq. (9.17), which remains unchanged, with the modified noise term given in Eq. (9.21). Hence the SNR for the APD is:

$$\frac{S}{N} = \frac{M^2 I_p^2}{2eB(I_p + I_d)M^{2+x} + \frac{4KTBF_n}{R_L}} \tag{9.22}$$

It is apparent from Eq. (9.22) that the relative significance of the combined thermal and amplifier noise term is reduced due to the avalanche multiplication of the shot noise term. When Eq. (9.22) is written in the form:

$$\frac{S}{N} = \frac{I_p^2}{2eB(I_p + I_d)M^x + \frac{4KTBF_n}{R_L}M^{-2}} \tag{9.23}$$

it may be seen that the first term in the denominator increases with increasing $M$ whereas the second term decreases. For low $M$ the combined thermal and amplifier noise term dominates and the total noise power is virtually unaffected when the signal level is increased, giving an improved SNR. However, when $M$ is large, the thermal and amplifier noise term becomes insignificant and the SNR decreases with increasing $M$ at the rate of $M^x$. An optimum value of the multiplication factor $M_{op}$ therefore exists which maximizes the SNR. It is given by:

$$\frac{2eB(I_p + I_d)\, M_{op}^x}{(4KTBF_n/R_L)\, M_{op}^{-2}} = \frac{2}{x} \tag{9.24}$$

and therefore:

$$M_{op}^{2+x} = \frac{4KTF_n}{xeR_L(I_p + I_d)} \tag{9.25}$$

The variation in $M_{op}$ for both silicon and germanium APDs is illustrated in Figure 9.5 [Ref. 5]. This shows a plot of Eq. (9.22) with $F_n$ equal to unity and neglecting the dark current. For good silicon APDs where $x$ is 0.3, the optimum multiplication factor covers a wide range. In the case illustrated in Figure 9.5, $M_{op}$ commences at about 40 where the possible improvement in SNR above a photodiode without internal gain is in excess of

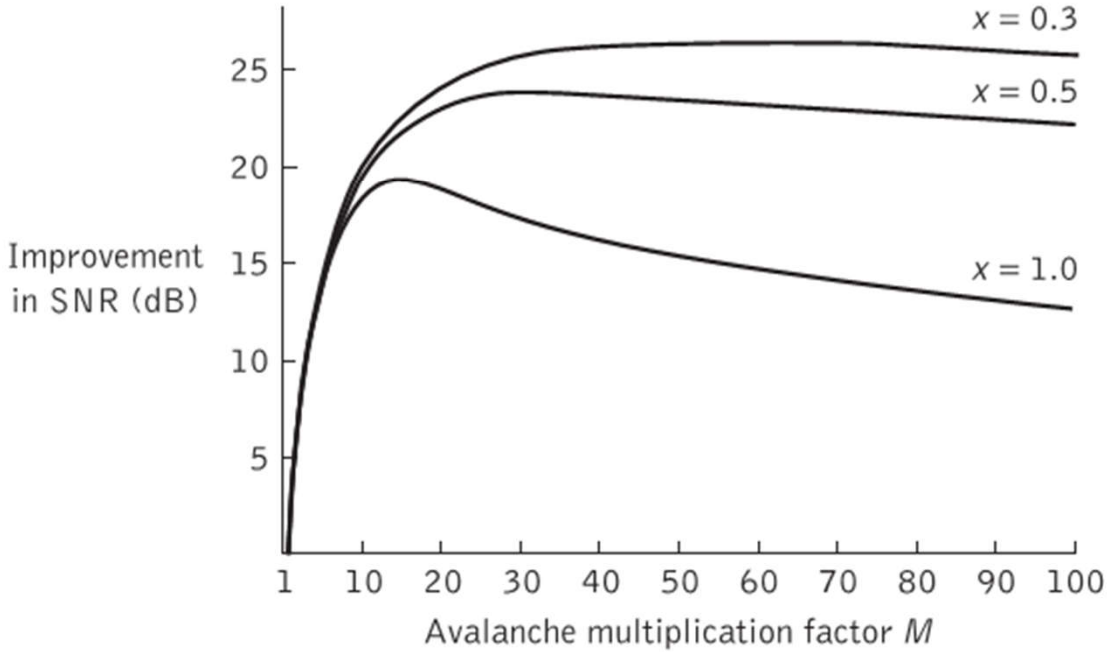


**Figure 9.5** The improvement in SNR as a function of avalanche multiplication factor $M$ for different excess noise factors $M^x$. Reproduced with permission from I. Garrett, *Radio Electron. Eng.*, **51**, p. 349, 1981

25 dB. However, for germanium and III–V alloy APDs where $x$ may be equal to unity, it can be seen that less SNR improvement is possible (less than 19 dB). Moreover, the maximum is far sharper, occurring at a multiplication factor of about 12. Also it must be noted that Figure 9.5 demonstrates the variation of $M_{op}$ with $x$ for a specific case, and therefore only represents a general trend. It may be observed from Eq. (9.25) that $M_{op}$ is dependent on a number of other variables apart from $x$.

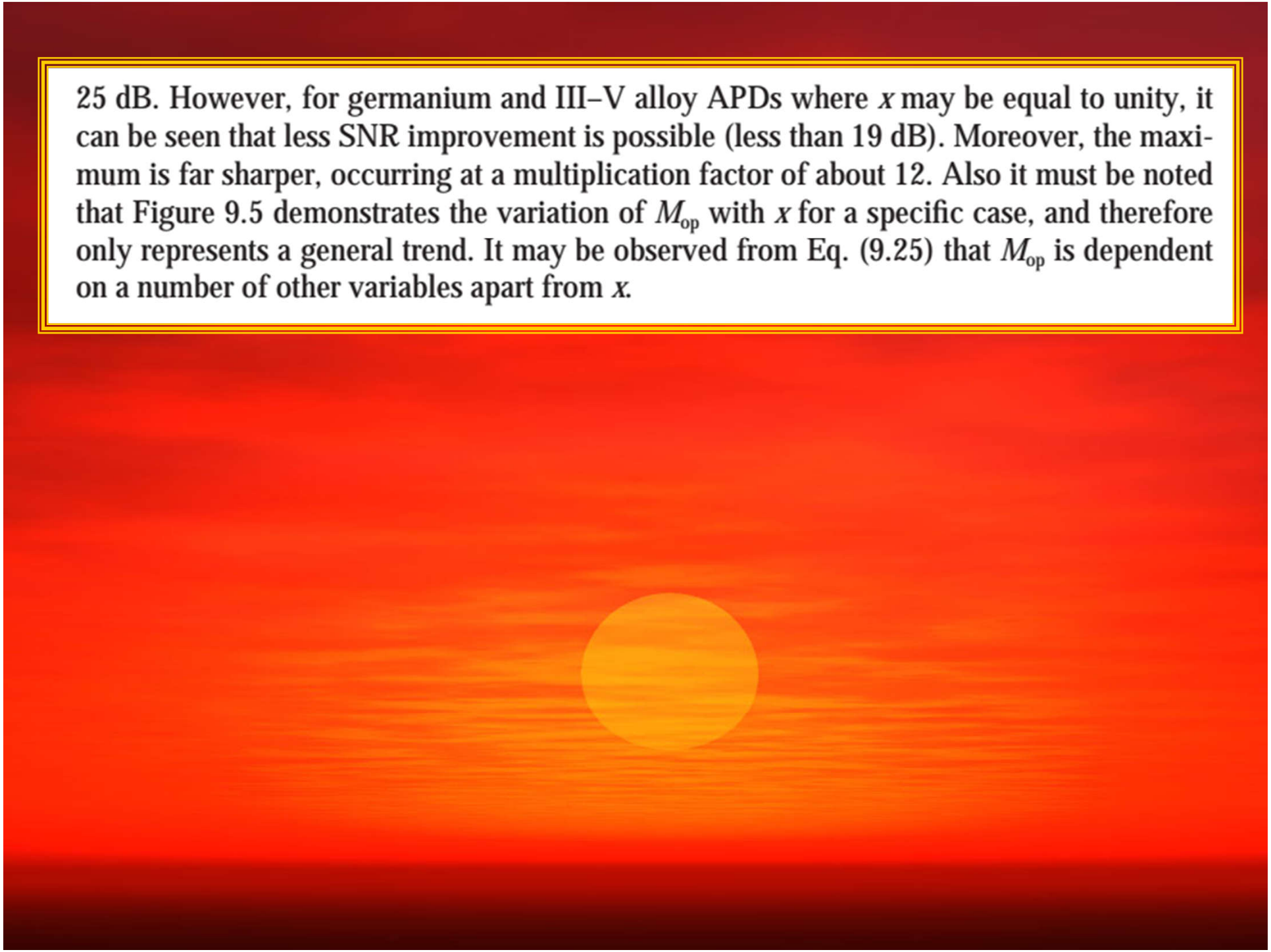

## Example 9.6

A good silicon APD ($x = 0.3$) has a capacitance of 5 pF, negligible dark current and is operating with a post-detection bandwidth of 50 MHz. When the photocurrent before gain is $10^{-7}$ A and the temperature is 18 °C, determine the maximum SNR improvement between $M = 1$ and $M = M_{op}$ assuming all operating conditions are maintained.

*Solution:* Determine the maximum value of the load resistor from Eq. (9.20):

$$R_L = \frac{1}{2\pi C_d B} = \frac{1}{2\pi \times 5 \times 10^{-12} \times 50 \times 10^6}$$

$$= 635.5\ \Omega$$

When $M = 1$, the SNR is given by Eq. (9.22):

$$\frac{S}{N} = \frac{I_p^2}{2eBI_p + \dfrac{4KTB}{R_L}}$$

where $I_d = 0$ and $F_n = 1$.

The shot noise is:

$$2eBI_p = 2 \times 1.602 \times 10^{-19} \times 50 \times 10^6 \times 10^{-7}$$
$$= 1.602 \times 10^{-18}\ \text{A}^2$$

and the thermal noise is:

$$\frac{4KTB}{R_L} = \frac{4 \times 1.381 \times 10^{-23} \times 291 \times 50 \times 10^6}{636.5}$$
$$= 1.263 \times 10^{-15}\ \text{A}^2$$

It may be noted that the thermal noise is dominating.
Therefore:

$$\frac{S}{N} = \frac{10^{-14}}{1.602 \times 10^{-18} \times 1.263 \times 10^{-15}} = 7.91$$

and the SNR in dB is:

$$\frac{S}{N} = 10 \log_{10} 7.91 = 8.98\ \text{dB}$$

Thus the SNR when $M = 1$ is 9.0 dB.
When $M = M_{op}$ and $x = 0.3$, from Eq. (9.25):

$$M_{\text{op}}^{2+x} = \frac{4KT}{xeR_L I_p}$$

where $I_d = 0$ and $F_n = 1$. Hence:

$$M_{\text{op}}^{2.3} = \frac{4 \times 1.381 \times 10^{-23} \times 291}{0.3 \times 1.602 \times 10^{-19} \times 636.5 \times 10^{-7}}$$

and:

$$\begin{aligned} M_{\text{op}} &= (5.255 \times 10^3)^{0.435} \\ &= 41.54 \end{aligned}$$

The SNR at $M_{\text{op}}$ may be obtained from Eq. (9.22):

$$\begin{aligned} \frac{S}{N} &= \frac{M^2 I_p^2}{2eBI_p M^{2.3} + \dfrac{4KTB}{R_L}} \\ &= \frac{(41.54)^2 \times 10^{-14}}{\{1.602 \times 10^{-18} \times (41.54)^{2.3}\} + 1.263 \times 10^{-15}} \\ &= 1.78 \times 10^3 \end{aligned}$$

and the SNR in dB is:

$$\frac{S}{N} = 10 \log_{10} 1.78 \times 10^3 = 32.50 \text{ dB}$$

Therefore the SNR when $M = M_{op}$ is 32.5 dB and the SNR improvement over $M = 1$ is 23.5 dB.

## Example 9.7

A germanium APD (with $x = 1$) is incorporated into an optical fiber receiver with a 10 kΩ load resistance. When operated at a temperature of 120 K, the minimum photocurrent required to give an SNR of 35 dB at the output of the receiver is found to be a factor of 10 greater than the dark current. If the noise figure of the following amplifier at this temperature is 1 dB and the post-detection bandwidth is 10 MHz, determine the optimum avalanche multiplication factor.

*Solution:* From Eq. (9.22) with $x = 1$ and $M = M_{op}$ (i.e. minimum photocurrent specifies that $M = M_{op}$) the SNR is:

$$\frac{S}{N} = \frac{M_{op}^2 I_p^2}{2eB(I_p + I_d)M_{op}^3 + \frac{4KTB}{R_L}}$$

Also from Eq. (9.25):

$$M_{op}^3 = \frac{4KTF_n}{eR_L(I_p + I_d)}$$

Therefore:

$$M_{op} = \left[ \frac{4KTF_n}{eR_L(I_p + I_d)} \right]^{\frac{1}{3}}$$

Substituting into Eq. (9.22), this gives:

$$\frac{S}{N} = \frac{\left[ \frac{4KTF_n}{eR_L(I_p + I_d)} \right]^{\frac{2}{3}} I_p^2}{\frac{8KTBF_n}{R_L} + \frac{4KTBF_n}{R_L}}$$

and as $I_d = 0.1I_p$ the SNR is:

$$\frac{S}{N} = \frac{\left(\frac{4KTF_n}{1.1eR_L}\right)^{\frac{2}{3}} I_p^{\frac{4}{3}}}{\frac{12KTBF_n}{R_L}}$$

Therefore the minimum photocurrent $I_p$:

$$I_p^{\frac{4}{3}} = \left(\frac{S}{N}\right) \frac{\frac{12KTBF_n}{R_L}}{\left(\frac{4KTF_n}{1.1eR_L}\right)^{\frac{2}{3}}}$$

where the SNR is:

$$\frac{S}{N} = 35 \text{ dB} = 3.16 \times 10^3$$

and as $F_n = 1$ dB which is equivalent to 1.26:

$$\frac{12KTBF_n}{R_L} = \frac{12 \times 1.381 \times 10^{-23} \times 120 \times 10^7 \times 1.26}{10^4}$$

$$= 2.51 \times 10^{-17}$$

Also:

$$\left(\frac{4KTF_{\mathrm{n}}}{1.1eR_{\mathrm{L}}}\right)^{\frac{1}{2}} = \left(\frac{4 \times 1.381 \times 10^{-23} \times 120 \times 1.26}{1.1 \times 1.602 \times 10^{-19} \times 10^{4}}\right)^{\frac{2}{3}}$$

$$= 2.82 \times 10^{-4}$$

Therefore:

$$I_{\mathrm{p}} = \left(\frac{3.16 \times 10^{3} \times 2.51 \times 10^{-17}}{2.82 \times 10^{-4}}\right)^{\frac{3}{4}}$$

$$= 6.87 \times 10^{-8}\ \mathrm{A}$$

To obtain the optimum avalanche multiplication factor we substitute back into Eq. (9.25), where:

$$M_{\mathrm{op}} = \left(\frac{4 \times 1.381 \times 10^{-23} \times 120 \times 1.26}{1.602 \times 10^{-19} \times 10^{3} \times 1.1 \times 6.87 \times 10^{-8}}\right)^{\frac{1}{3}}$$

$$= 8.84$$

In Example 9.7 the optimum multiplication factor for the germanium APD is found to be approximately 9. It shows the dependence of the optimum multiplication factor on the variables in Eq. (9.25), and although the example does not necessarily represent a practical receiver (some practical germanium APD receivers are cooled to reduce dark current), the optimum multiplication factor is influenced by device and system parameters as well as operating conditions.

## 9.3.4 Excess avalanche noise factor

The value of the excess avalanche noise factor is dependent upon the detector material, the shape of the electric field profile within the device and whether the avalanche is initiated by holes or electrons. It is often represented as $F(M)$ and in the preceding section we have considered one of the approximations for the excess noise factor, where:

$$F(M) = M^x \tag{9.26}$$

and the resulting noise is assumed to be white with a Gaussian distribution.

However, a second and more exact relationship is given by [Ref. 6]:

$$F(M) = M\left[1 - (1-k)\left(\frac{M-1}{M}\right)^2\right] \tag{9.27}$$

where the only carriers are injected electrons and $k$ is the ratio of the ionization coefficients of holes and electrons. If the only carriers are injected holes:

$$F(M) = M\left[1 + \left(\frac{1-k}{k}\right)\left(\frac{M-1}{M}\right)^2\right] \tag{9.28}$$

Figure 9.6 provides the excess avalanche noise factor as a function of multiplication factor $M$ for several values of $k$ which is obtained from Eq. (9.28). It should be noted that the hole injections for a value of $k = 1$, the excess noise factor, are simply equal to the multiplication factor. In the case of holes the smaller values of $k$ produce high performance and therefore the best performance is achieved when $k$ is small. Moreover, for silicon APDs $k$ is between 0.02 and 0.10, whereas for germanium and III–V alloy APDs $k$ is between 0.3 and 1.0.

With electron injection in silicon photodiodes, the smaller values of $k$ obtained correspond to a larger ionization rate for the electrons than for the holes. As $k$ departs from unity, only the carrier with the larger ionization rate contributes to the impact ionization and the excess avalanche noise factor is reduced. When the impact ionization is initiated by electrons this corresponds to fewer ionizing collisions involving the hole current which is flowing in the opposite direction (i.e. less feedback). In this case the amplified signal contains less excess noise. The carrier ionization rates in germanium photodiodes are often nearly equal and hence $k$ approaches unity, giving a high level of excess noise.

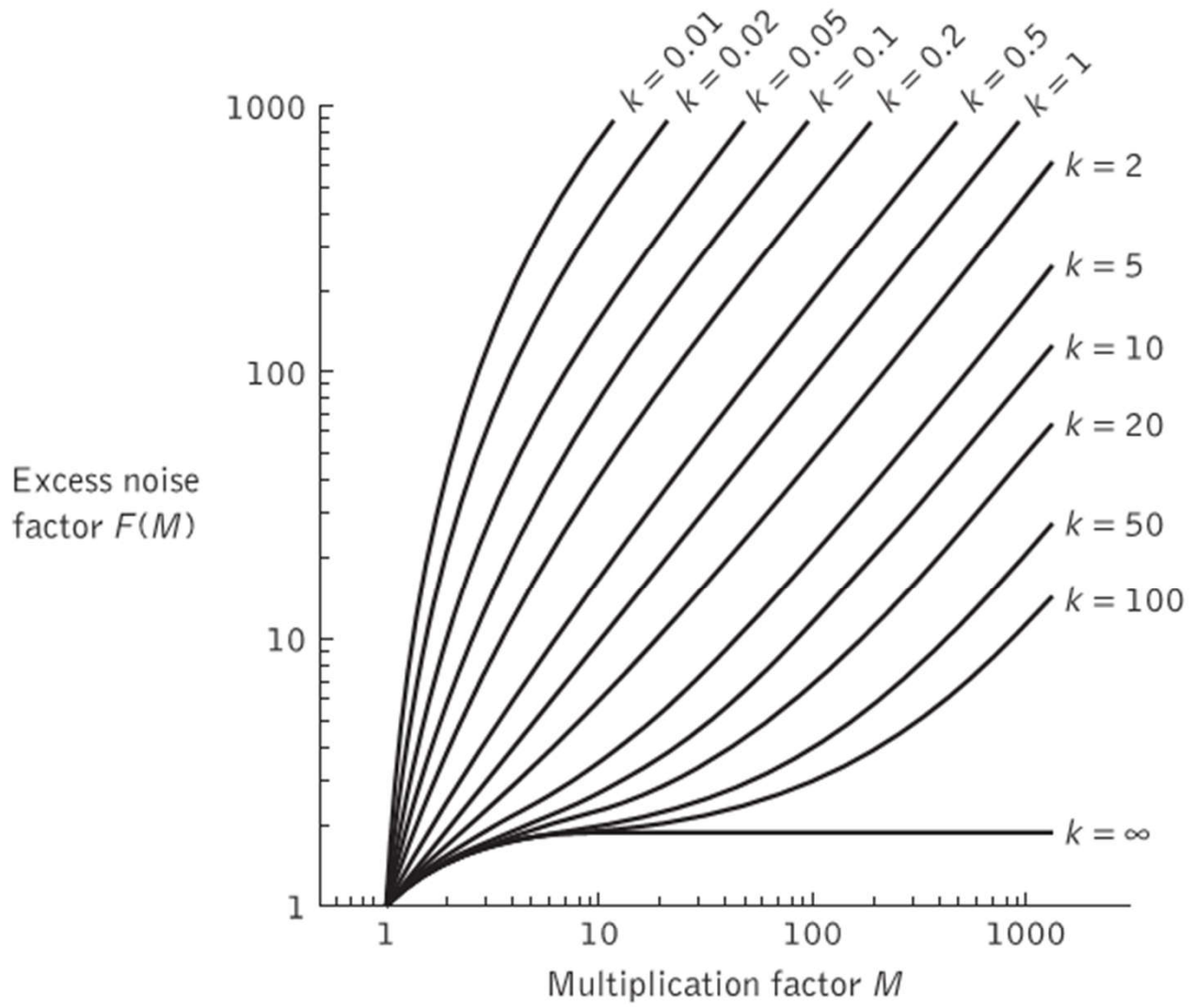


**Figure 9.6** Excess noise factor against multiplication factor for different values of the ratio of ionization coefficients for holes and electrons $k$; hole injection based on Eq. (9.28).

## 9.3.5 Gain-bandwidth product

In addition to SNR a figure of merit for an APD receiver can also be expressed in terms of either the maximum 3 dB bandwidth or, alternatively, the gain–bandwidth product [Ref. 7]. The latter term is defined as gain multiplied by the bandwidth and determines a higher transmission rate limit related to the gain of the APD device. Since gain is a dimensionless quantity the gain–bandwidth product is therefore measured in the units of frequency (i.e. GHz).

Figure 9.7 shows the relationship between bandwidth and multiplication factor of an APD [Ref. 8]. The circles represent the 3 dB bandwidth values and constitute a nonlinear curve containing a linear part at higher values of the multiplication factor. The linearity occurs at a cut off frequency point after which the gain of the APD remains constant (i.e. in this particular case, at $M > 6$). When these point values displaying the linear part are connected as indicated in the Figure 9.7, the resultant slope line represents the theoretical value of the achievable gain–bandwidth product for an APD. For example, the 3 dB bandwidth at $M = 10$ remains 14 GHz which produces a gain–bandwidth product of 140 GHz. Furthermore, it maintains the same value of gain–bandwidth product for $M = 6$ with a 3 dB bandwidth of 23.3 GHz. This suggests a theoretical limit for the gain–bandwidth product of 140 GHz for the same device. The maximum 3 dB bandwidth for the APD, however, is shown as 40 GHz which is identified by the horizontal dashed line in Figure 9.7.

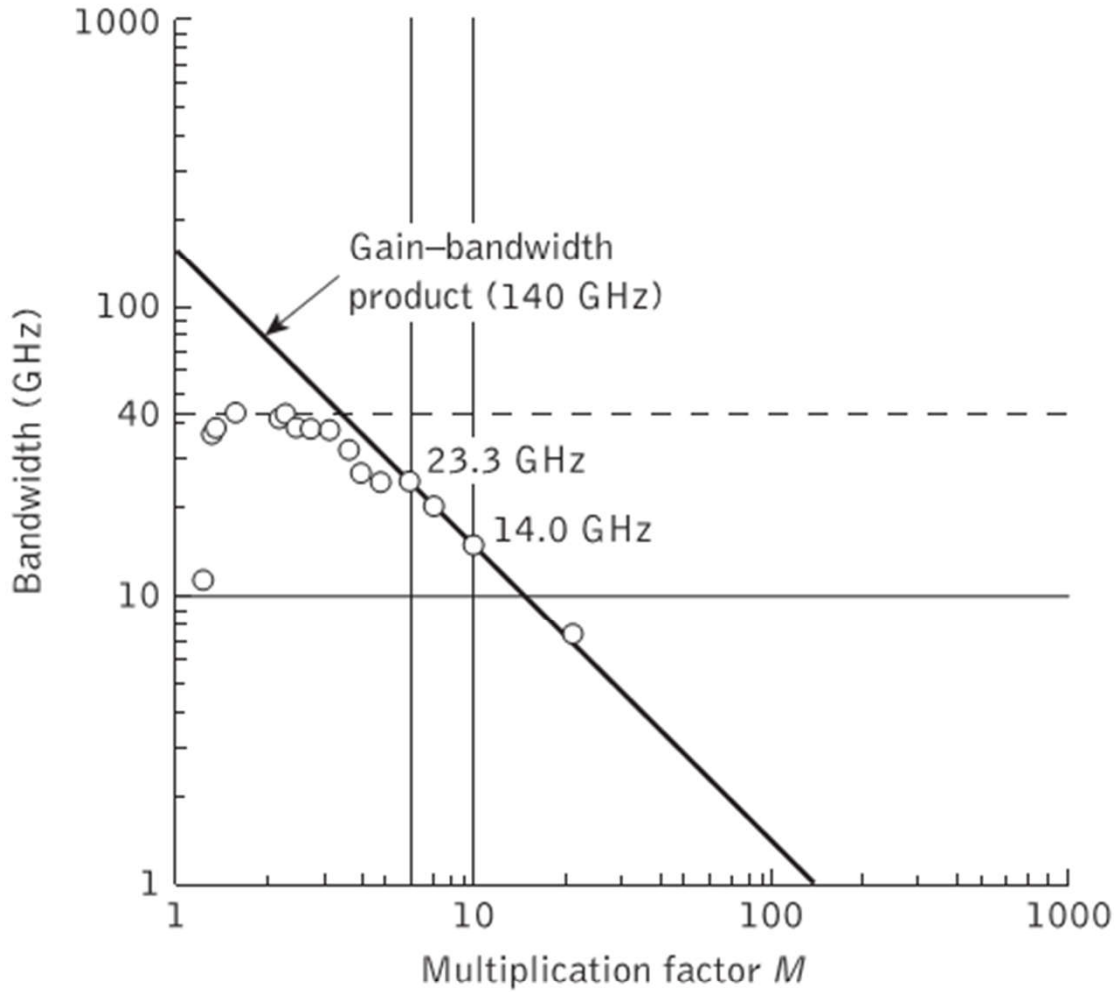


**Figure 9.7** Bandwidth (3 dB) against multiplication factor for an APD; adapted with permission from Ref. 8 © IEEE 2004

Silicon APDs are recognized for their high gain–bandwidth products which result from the large asymmetry of electron and hole ionization coefficients leading to a ratio of ionization coefficients $k$ of around 50 [Ref. 9]. However, these APDs do not operate at signal wavelengths between 1.3 and 1.6 μm and therefore they are not preferred for use in receivers operating at high transmission rates. Although InGaAs/InP-based APDs possess high quantum efficiency and can be utilized at signal wavelengths between 1.3 and 1.6 μm, they suffer from a lower gain–bandwidth product due to the small ratios of ionization coefficients in InP. Nevertheless, separate absorption, charge and multiplication (SACM) APD receivers (see Section 8.9.4) based on the InGaAs/InAlAs material system exhibit large gain–bandwidth products and a 290 GHz gain–bandwidth for such APDs has been achieved while maintaining the 3 dB bandwidth at 33 GHz [Ref. 10]. Hence such devices have found application in high-speed optical receivers where they provide greater sensitivity in comparison with *p–i–n* photodiodes.

## 9.4 Receiver structures

A full equivalent circuit for the digital optical fiber receiver, in which the optical detector is represented as a current source $i_{det}$, is shown in Figure 9.8. The noise sources ($i_t$, $i_{TS}$ and $i_{amp}$) and the immediately following amplifier and equalizer are also shown. Equalization [Ref. 11] compensates for distortion of the signal due to the combined transmitter, medium and receiver characteristics. The equalizer is often a frequency-shaping filter which has a frequency response that is the inverse of the overall system frequency response. In wideband systems this will normally boost the high-frequency components to correct the overall

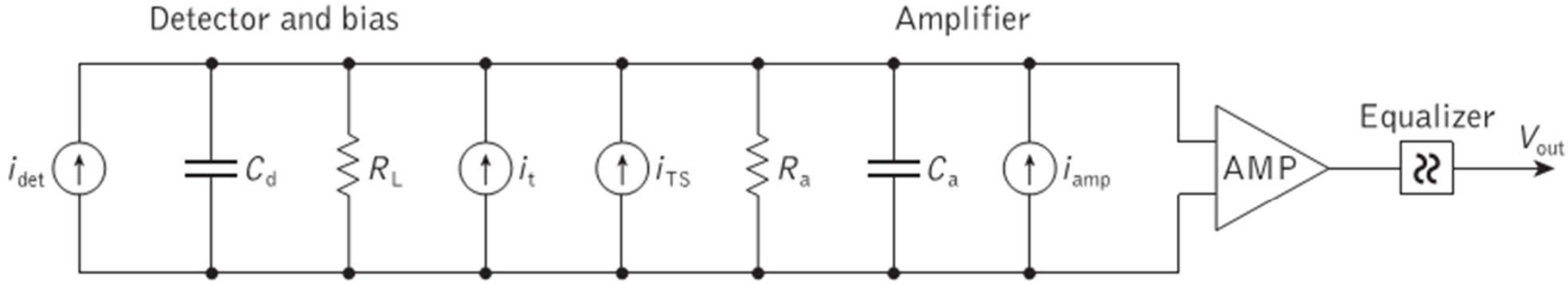


**Figure 9.8** A full equivalent circuit for a digital optical fiber receiver including the various noise sources

amplitude of the frequency response. To acquire the desired spectral shape for digital systems (e.g. raised cosine, see Figure 12.39), in order to minimize intersymbol interference, it is important that the phase frequency response of the system is linear. Thus the equalizer may also apply selective phase shifts to particular frequency components.

However, the receiver structure immediately preceding the equalizer is the major concern of this section. In both digital and analog systems it is important to minimize the noise contributions from the sources shown in Figure 9.8 so as to maximize the receiver sensitivity while maintaining a suitable bandwidth. It is therefore useful to discuss various possible receiver structures with regard to these factors.

## 9.4.1 Low-impedance front-end

Three basic amplifier configurations are frequently used in optical fiber communication receivers. The simplest, and perhaps the most common, is the voltage amplifier with an effective input resistance $R_a$ as shown in Figure 9.9. In order to make suitable design choices, it is necessary to consider both bandwidth and noise. The bandwidth considerations in Section 9.3.2 are treated solely with regard to a detector load resistance $R_L$. However, in most practical receivers the detector is loaded with a bias resistor $R_b$ and an amplifier (see Figure 9.9). The bandwidth is determined by the passive impedance which appears across the detector terminals which is taken as $R_L$ in the bandwidth relationship given in Eq. (9.20).

However, $R_L$ may be modified to incorporate the parallel resistance of the detector bias resistor $R_b$ and the amplifier input resistance $R_a$. The modified total load resistance $R_{TL}$ is therefore given by:

$$R_{TL} = \frac{R_b R_a}{R_b + R_a} \tag{9.29}$$

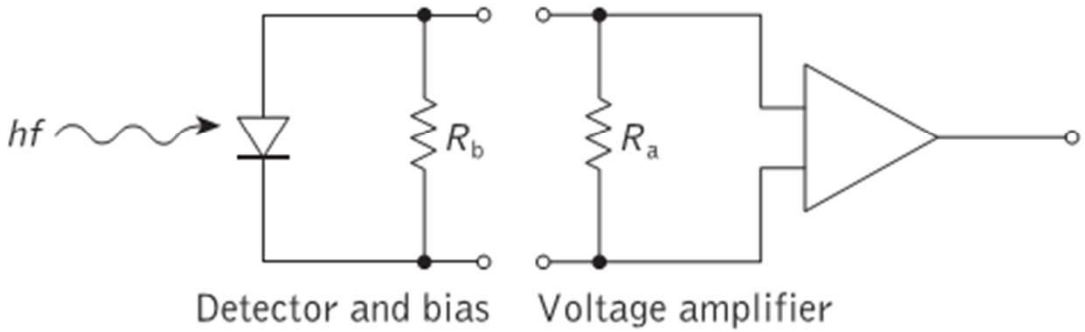


**Figure 9.9** Low-impedance front-end optical fiber receiver with voltage amplifier

Considering the expressions given in Eqs (9.20) and (9.29), to achieve an optimum bandwidth both $R_b$ and $R_a$ must be minimized. This leads to a low-impedance front-end design for the receiver amplifier. Unfortunately this design allows thermal noise to dominate within the receiver (following Eq. (9.14)), which may severely limit its sensitivity. Therefore this structure demands a trade-off between bandwidth and sensitivity which tends to make it impractical for long-haul, wideband optical fiber communication systems.

## 9.4.2 High-impedance (integrating) front-end

The second configuration consists of a high input impedance amplifier together with a large detector bias resistor in order to reduce the effect of thermal noise. However, this structure tends to give a degraded frequency response as the bandwidth relationship given in Eq. (9.20) is not maintained for wideband operation. The detector output is effectively integrated over a large time constant and must be restored by differentiation. This may be performed by the correct equalization at a later stage [Ref. 12] as illustrated in Figure 9.10. Therefore the high-impedance (integrating) front-end structure gives a significant improvement in sensitivity over the low-impedance front-end design, but it creates a heavy demand for equalization and has problems of limited dynamic range (the ratio of maximum to minimum input signals).

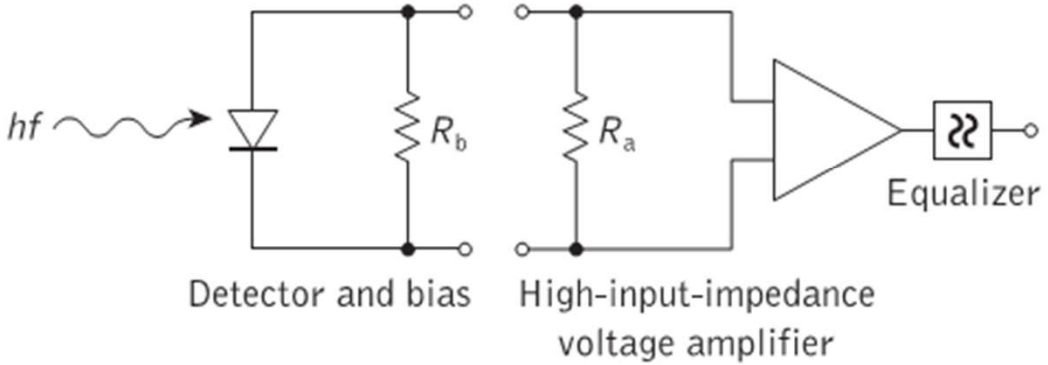


**Figure 9.10** High-impedance integrating front-end optical fiber receiver with equalized voltage amplifier

The limitations on dynamic range result from the attenuation of the low-frequency signal components by the equalization process which causes the amplifier to saturate at high signal levels. When the amplifier saturates before equalization has occurred, the signal is heavily distorted. Thus the reduction in dynamic range is dependent upon the amount of integration and subsequent equalization employed.

## 9.4.3 The transimpedance front-end

This configuration largely overcomes the drawbacks of the high-impedance front end by utilizing a low-noise, high-input-impedance amplifier with negative feedback. The device therefore operates as a current mode amplifier where the high input impedance is reduced by negative feedback. An equivalent circuit for an optical fiber receiver incorporating a transimpedance front-end structure is shown in Figure 9.11. In this equivalent circuit the parallel resistances and capacitances are combined into $R_{TL}$ and $C_T$ respectively. The open loop current to voltage transfer function $H_{OL}$ $(\omega)$ for this transimpedance configuration

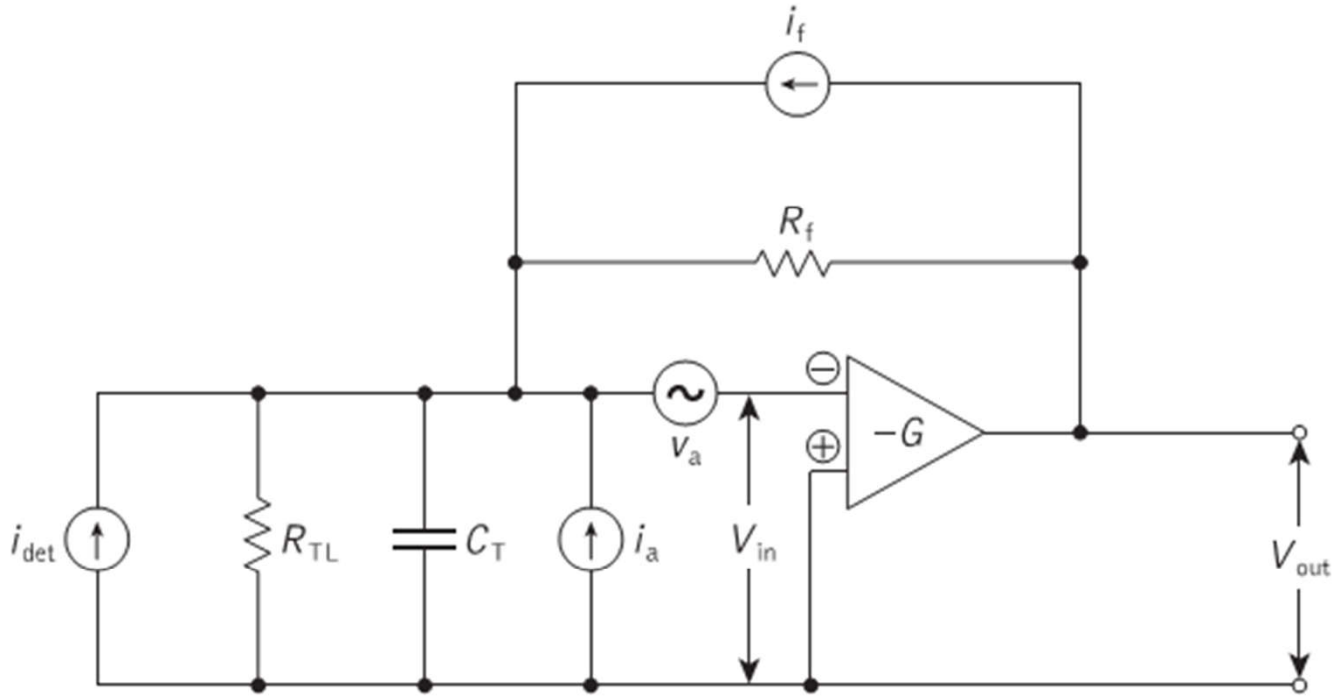


**Figure 9.11** An equivalent circuit for the optical fiber receiver incorporating a transimpedance (current mode) preamplifier

corresponds to the transfer function for the two structures described previously which do not employ feedback (i.e. the low- and high-impedance front ends). It may be written as:

$$H_{OL}(\omega) = -G\frac{V_{in}}{i_{det}} = -G\frac{R_{TL}\dfrac{1}{j\omega C_T}}{R_{TL}+\dfrac{1}{j\omega C_T}} = \frac{-GR_{TL}}{1+j\omega R_{TL}C_T}\ (\mathrm{V\ A^{-1}}) \tag{9.30}$$

where $G$ is the open loop voltage gain of the amplifier and $\omega$ is the angular frequency of the input signal. In this case the bandwidth (without equalization) is constrained by the time constant given in Eq. (9.20).*

When the feedback is applied, the closed loop current to voltage transfer function $H_{CL}(\omega)$ for the transimpedance configuration is given by (see Appendix E):

$$H_{CL}(\omega) \simeq \frac{-R_f}{1+(j\omega R_f C_T/G)}\ (\mathrm{V\ A^{-1}}) \tag{9.31}$$

where $R_f$ is the value of the feedback resistor. In this case the permitted electrical bandwidth $B$ (without equalization) may be written as:

$$B \leq \frac{G}{2\pi R_f C_T} \tag{9.32}$$

Hence, comparing Eq. (9.32) with Eq. (9.20) it may be noted that the transimpedance (or feedback) amplifier provides a much greater bandwidth than do the amplifiers without feedback. This is particularly pronounced when $G$ is large.

* The time constant can be obtained directly from Eq. (9.30) where the maximum bandwidth is defined by $\omega = 2\pi B = 1/R_{TL}C_T$.

Moreover, it is interesting to consider the thermal noise generated by the transimpedance front end. Using a referred impedance noise analysis it can be shown [Ref. 13] that to a good approximation the feedback resistance (or impedance) may be referred to the amplifier input in order to establish the noise performance of the configuration. Thus when $R_f \ll R_{TL}$, the major noise contribution is from thermal noise generated in $R_f$. The noise performance of this configuration is therefore improved when $R_f$ is large, and it approaches the noise performance of the high-impedance front end when $R_f = R_{TL}$. Unfortunately, the value of $R_f$ cannot be increased indefinitely due to problems of stability with the closed loop design. Furthermore, it may be observed from Eq. (9.32) that increasing $R_f$ reduces the bandwidth of the transimpedance configuration. This problem may be alleviated by making $G$ as large as the stability of the closed loop will allow. Nevertheless, it is clear that the noise in the transimpedance amplifier will always exceed that incurred by the high-impedance front-end structure.

## Example 9.8

A high-input-impedance amplifier which is employed in an optical fiber receiver has an effective input resistance of 4 MΩ which is matched to a detector bias resistor of the same value. Determine:

(a) The maximum bandwidth that may be obtained without equalisation if the total capacitance $C_T$ is 6 pF.

(b) The mean square thermal noise current per unit bandwidth generated by this high-input-impedance amplifier configuration when it is operating at a temperature of 300 K.

(c) Compare the values calculated in (a) and (b) with those obtained when the high-input-impedance amplifier is replaced by a transimpedance amplifier with a 100 kΩ feedback resistor and an open loop gain of 400. It may be assumed that $R_f \ll R_{TL}$, and that the total capacitance remains 6 pF.

*Solution:* (a) Using Eq. (9.29), the total effective load resistance:

$$R_{TL} = \frac{(4 \times 10^6)^2}{8 \times 10^6} = 2 \text{ M}\Omega$$

Hence from Eq. (9.20) the maximum bandwidth is given by:

$$B = \frac{1}{2\pi R_{TL} C_T} = \frac{1}{2\pi \times 2 \times 10^6 \times 6 \times 10^{-12}}$$

$$= 1.33 \times 10^4 \text{ Hz}$$

The maximum bandwidth that may be obtained without equalization is 13.3 kHz.

(b) The mean square thermal noise current per unit bandwidth for the high-impedance configuration following Eq. (9.14) is:

$$\overline{i_t^2} = \frac{4KT}{R_{TL}} = \frac{4 \times 1.381 \times 10^{-23} \times 300}{2 \times 10^6}$$

$$= 8.29 \times 10^{-27} \text{ A}^2 \text{ Hz}^{-1}$$

(c) The maximum bandwidth (without equalization) for the transimpedance configuration may be obtained using Eq. (9.32), where:

$$B = \frac{G}{2\pi R_f C_T} = \frac{400}{2\pi \times 10^5 \times 6 \times 10^{-12}}$$

$$= 1.06 \times 10^8 \text{ Hz}$$

Hence a bandwidth of 106 MHz is permitted by the transimpedance design.

Assuming $R_f \ll R_{TL}$, the mean square thermal noise current per unit bandwidth for the transimpedance configuration is given by:

$$\overline{i_t^2} = \frac{4KT}{R_f} = \frac{4 \times 1.381 \times 10^{-23} \times 300}{10^5}$$

$$= 1.66 \times 10^{-25} \text{ A}^2 \text{ Hz}^{-1}$$

The mean square thermal noise current in the transimpedance configuration is therefore a factor of 20 greater than that obtained with the high-input-impedance configuration.

The equivalent value in decibels of the ratio of these noise powers is:

$$\frac{\text{Noise power in the transimpedance configuration}}{\text{Noise power in the high-input-impedance configuration}} = 10 \log_{10} 20$$

$$= 13 \text{ dB}$$

Thus the transimpedance front-end in Example 9.8 provides a far greater bandwidth without equalization than the high-impedance front-end. However, this advantage is somewhat offset by the 13 dB noise penalty incurred with the transimpedance amplifier over that of the high-input-impedance configuration. Nevertheless it is apparent, even from this simple analysis, that transimpedance amplifiers may be optimized for noise performance, although this is usually obtained at the expense of bandwidth. This topic is pursued further in Ref. 14. However, wideband transimpedance designs generally give a significant improvement in noise performance over the low-impedance front-end structures using simple voltage amplifiers (see Problem 9.18). Finally it must be emphasized that the approach adopted in Example 9.8 is by no means rigorous and includes two important simplifications:

firstly, that the thermal noise in the high-impedance amplifier is assumed to be totally generated by the effective input resistance of the device; and secondly, that the thermal noise in the transimpedance configuration is assumed to be totally generated by the feedback resistor when it is referred to the amplifier input. Both these assumptions are approximations, the accuracy of which is largely dependent on the parameters of the particular amplifier. For example, another factor which tends to reduce the bandwidth of the transimpedance amplifier is the stray capacitance $C_f$ generally associated with the feedback resistor $R_f$. When $C_f$ is taken into account the closed loop response of Eq. (9.31) becomes:

$$H_{CL}(\Omega) \simeq \frac{-R_f}{1 + j\omega R_f(C_T/G + C_f)} \tag{9.33}$$

However, the effects of $C_f$ may be cancelled by employing a suitable compensating network [Ref. 15].

The other major advantage which the transimpedance configuration has over the high-impedance front end is a greater dynamic range. This improvement in dynamic range obtained using the transimpedance amplifier is a result of the different attenuation mechanism for the low-frequency components of the signal. The attenuation is accomplished in the transimpedance amplifier through the negative feedback and therefore the low-frequency components are amplified by the closed loop rather than the open loop gain of the device. Hence for a particular amplifier the improvement in dynamic range is approximately equal to the ratio of the open loop to the closed loop gains. The transimpedance structure therefore overcomes some of the problems encountered with the other configurations and is often preferred for use in wideband optical fiber communication receivers [Ref. 16].

## 9.5 FET preamplifiers

The lowest noise amplifier device which is widely available is the silicon FET. Unlike the bipolar transistor, the FET operates by controlling the current flow with an electric field produced by an applied voltage on the gate of the device (see Figure 9.12) rather than with

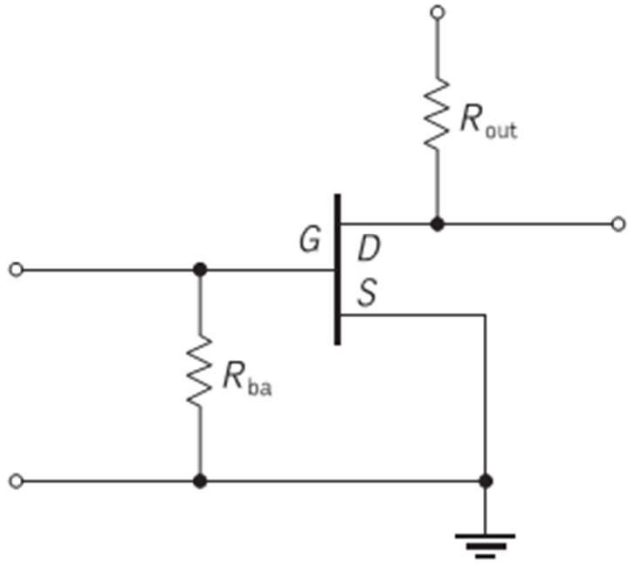


**Figure 9.12** Grounded source FET configuration for the front end of an optical fiber receiver amplifier

a base current. Thus the gate draws virtually no current, except for leakage, giving the device an extremely high input impedance (can be greater than $10^{14}$ ohms). This, coupled with its low noise and capacitance (no greater than a few picofarads), makes the silicon FET appear an ideal choice for the front end of the optical fiber receiver amplifier. However, the superior properties of the FET over the bipolar transistor are limited by its comparatively low transconductance $g_m$ (no better than 5 millisiemens in comparison with at least 40 millisiemens for the bipolar). It can be shown [Ref. 14] that a figure of merit with regard to the noise performance of the FET amplifier is $g_m/C_T^2$. Hence the advantage of high transconductance together with low total capacitance $C_T$ is apparent. Moreover, as $C_T = C_d + C_a$, it should be noted that the figure of merit is optimized when $C_a = C_d$. This requires FETs to be specifically matched to particular detectors, a procedure which device availability does not generally permit in current optical fiber receiver design. As indicated above, the gain of the FET is restricted. This is especially the case for silicon FETs at frequencies above 25 MHz where the current gain drops to values near unity as the transconductance is fixed with a decreasing input impedance. Therefore at frequencies above 25 MHz, the bipolar transistor is a more useful amplifying device.*

Figure 9.12 shows the grounded source FET configuration which increases the device input impedance especially if the amplifier bias resistor $R_{ba}$ is large. A large bias resistor has the effect of reducing the thermal noise but it will also increase the low-frequency impedance of the detector load which tends to integrate the signal (i.e. high-impedance integrating front-end). Thus compensation through equalization at a later stage is generally required.

## 9.5.1 Gallium arsenide MESFETs

Although silicon FETs have a limited useful bandwidth, much effort has been devoted to the development of high-performance microwave FETs since the mid-1970s. These FETs are fabricated from gallium arsenide and, being Schottky barrier devices [Refs 17–20], are called GaAs metal Schottky field effect transistors (MESFETs). They overcome the major disadvantage of silicon FETs in that they will operate with both low noise and high gain at microwave frequencies (GHz). Thus in optical fiber communication receiver design they present an alternative to bipolar transistors for wideband operation. These devices have therefore been incorporated into high-performance receiver designs using both *p–i–n* and detectors [Refs 21–32] . In particular, there has been much interest in hybrid integrated receiver circuits utilizing *p–i–n* photodiodes with GaAs MESFET amplifier front ends. The hybrid integration of a photodetector with a GaAs MESFET preamplifier having low leakage current, low capacitance (less than 0.5 pF) and high transconductance (greater than 30 millisiemens) provides a strategy for low-noise optical receiver design [Ref. 33].

* The figure of merit in relation to noise performance for the bipolar transistor amplifier may be shown [Ref. 14] to be $(h_{FE})^{\frac{1}{2}}/C_T$ where $h_{FE}$ is the common emitter current gain of the device. Hence the noise performance of the bipolar amplifier may be optimized in a similar manner to that of the FET amplifier.

## 9.5.2 PIN–FET hybrid receivers

The *p–i–n*/FET, or PIN–FET, hybrid receiver utilizes a high-performance *p–i–n* photodiode followed by a low-noise preamplifier often based on a GaAs MESFET, the whole of which is fabricated using thick-film integrated circuit technology. This hybrid integration on a thick-film substrate reduces the stray capacitance to negligible levels giving a total input capacitance which is very low (e.g. 0.4 pF). The MESFETs employed have a transconductance of approximately 15 millisiemens at the bandwidths required (e.g. 40 $Gbits^{-1}$ [Ref. 31]). Early work [Refs 22, 23] in the 0.8 to 0.9 μm wavelength band utilizing a silicon *p–i–n* detector showed the PIN–FET hybrid receiver to have a sensitivity of −45.8 dBm for a $10^{-9}$ BER which is only 4 dB worse than current silicon RAPD receivers (see Section 8.9.2).

The work was subsequently extended into the longer wavelength band (1.1 to 1.6 μm) utilizing III–V alloy *p–i–n* photodiode detectors. An example of a PIN–FET hybrid high-impedance (integrating) front-end receiver for operation at a wavelength of 1.3 μm using an InGaAs *p–i–n* photodiode is shown in Figure 9.13 [Refs 24–27]. This design, used by British Telecom, consists of a preamplifier with a GaAs MESFET and microwave bipolar transistor cascode followed by an emitter follower output buffer. The cascode circuit is chosen to ensure that sufficient gain is obtained from the first stage to give an overall gain of 18 dB. As the high-impedance front end effectively integrates the signal, the following digital equalizer is necessary. The pulse shaping and noise filtering circuits comprise two passive filter sections to ensure that the pulse waveform shape is optimized and the noise is minimized. Equalization for the integration (i.e. differentiation) is performed by monitoring the change in the integrated waveform over one period with a subminiature coaxial delay line followed by a high-speed, low-level comparator. The receiver is designed for use at a transmission rate of 140 Mbit $s^{-1}$ where its performance is found to be comparable to germanium and III–V alloy APD receivers. For example, the receiver sensitivity at a BER of $10^{-9}$ is −44.2 dBm. Table 9.1 provides a comparison of typical sensitivities

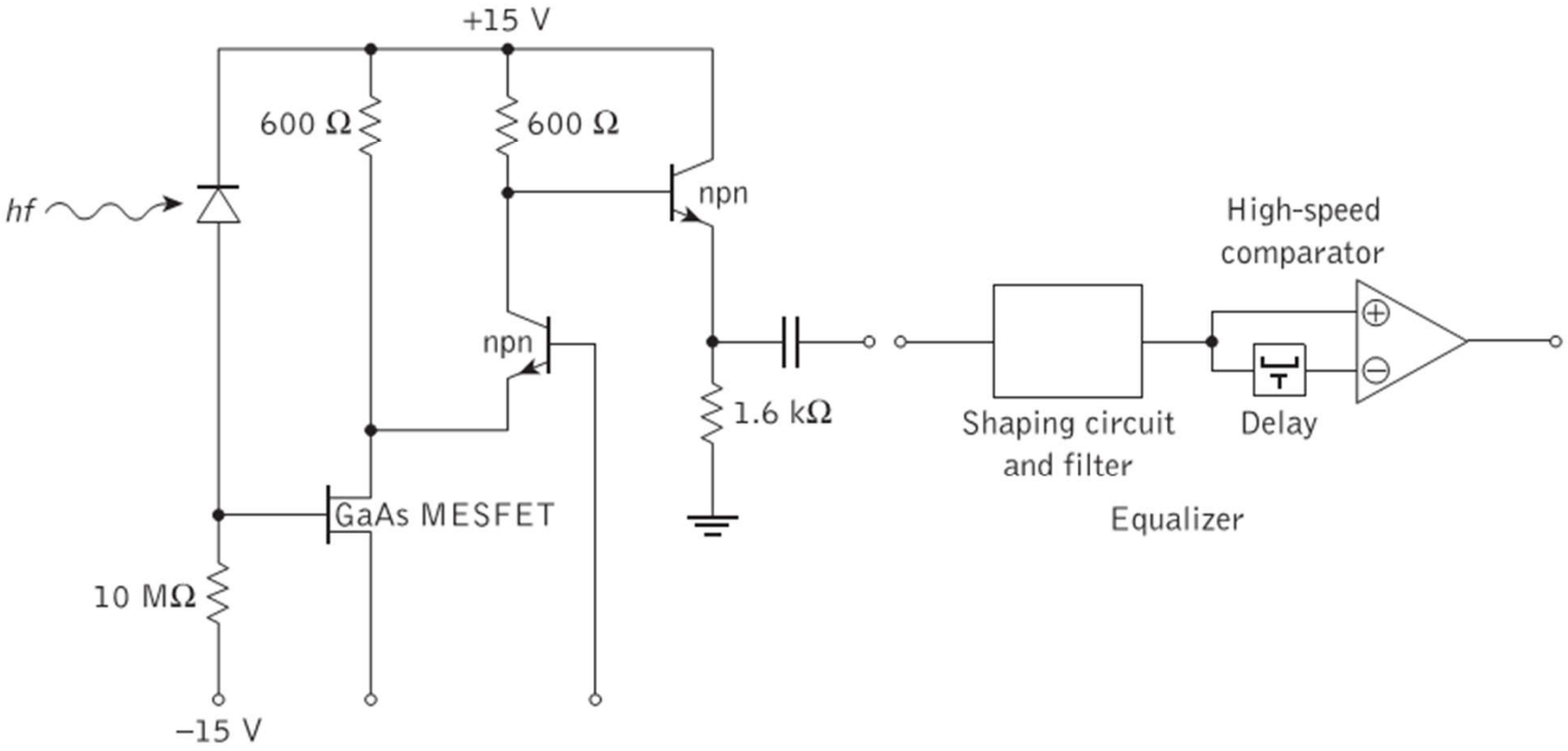


**Figure 9.13** PIN–FET hybrid high-impedance integrating front-end receiver [Refs 24–27]

**Table 9.1** Sensitivities for InGaAs PIN–FET and InAlAs APD receivers at the wavelength of 1.55 μm

| *Receiver type* | *Sensitivity (dBm)* | *Transmission rate (Gbit $s^{-1}$)* | *References* |
|---|---|---|---|
| PIN–FET | –23.0 | 2.5 | [Ref. 34] |
| APD | –34.0 | 2.5 | [Ref. 34] |
| APD | –29.0 | 10 | [Ref. 35] |
| APD | –27.1 | 10 | [Ref. 36] |
| PIN–FET | –7.0 | 40 | [Ref. 34] |

obtained with an InGaAs hybrid PIN–FET receiver and an InAlAs APD receiver when both are operating at a wavelength of 1.55 μm. The hybrid PIN–FET receiver design displays a lower sensitivity than the APD receiver at a transmission rate of 2.5 Gbit $s^{-1}$ and although it can also function at the higher transmission rate of 40 Gbit $s^{-1}$, the PIN–FET receiver then exhibits a very poor sensitivity of only −7.0 dBm [Ref. 34]. It should be noted that it is difficult to achieve higher transmission rates using conventional PIN–FET or APD receivers due to limitations in their gain–bandwidth products. Furthermore, the trade-off between the multiplication factor requirement and the maximum 3 dB bandwidth also limits the performance of the conventional receivers. However, incorporating optical amplifiers into traveling-waveguide (TW) and unitraveling carrier (UTC) structures (see Section 8.9.4) facilitates the design of photoreceivers capable of operating at transmission rates higher than 40 Gbit $s^{-1}$ [Ref. 8] (also see Section 9.6).

When compared with the APD receiver the PIN–FET hybrid has both cost and operational advantages especially in the longer wavelength region. The low-voltage operation (e.g. +15 and −15 V supply rails) coupled with good sensitivity and ease of fabrication makes the incorporation of this receiver into wideband optical fiber communication systems commercially attractive. A major drawback with the PIN–FET receiver is the possible lack of dynamic range. However, the configuration shown in Figure 9.13 gave adequate dynamic range via a control circuit which maintained the mean voltage at the gate at 0 V by applying a negative voltage proportional to the mean photocurrent to the MESFET bias resistor. With a −15 V supply rail an optical dynamic range of some 20 dB was obtained. This was increased to 27 dB by reducing the value of the MESFET bias resistor from 10 to 2 MΩ which gave a slight noise penalty of 0.5 dB. These figures compare favorably with practical APD receivers.

Transimpedance front-end receivers have also been fabricated using the PIN–FET hybrid approach. An example of this type of circuit [Ref. 29] is shown in Figure 9.14. The amplifier consists of a GaAs MESFET followed by two complementary bipolar microwave transistors. A silicon *p–i–n* photodiode was utilized with the amplifier and the receiver was designed to accept data at a rate of 274 Mbits $s^{-1}$. In this case the effective input capacitance of the receiver was 4.5 pF giving a sensitivity around −35 dBm for a BER of $10^{-9}$.

These figures are somewhat worse than the high-impedance front-end design discussed previously. However, this design has the distinct advantage of a flat frequency response to a wider bandwidth which requires little, if any, equalization.

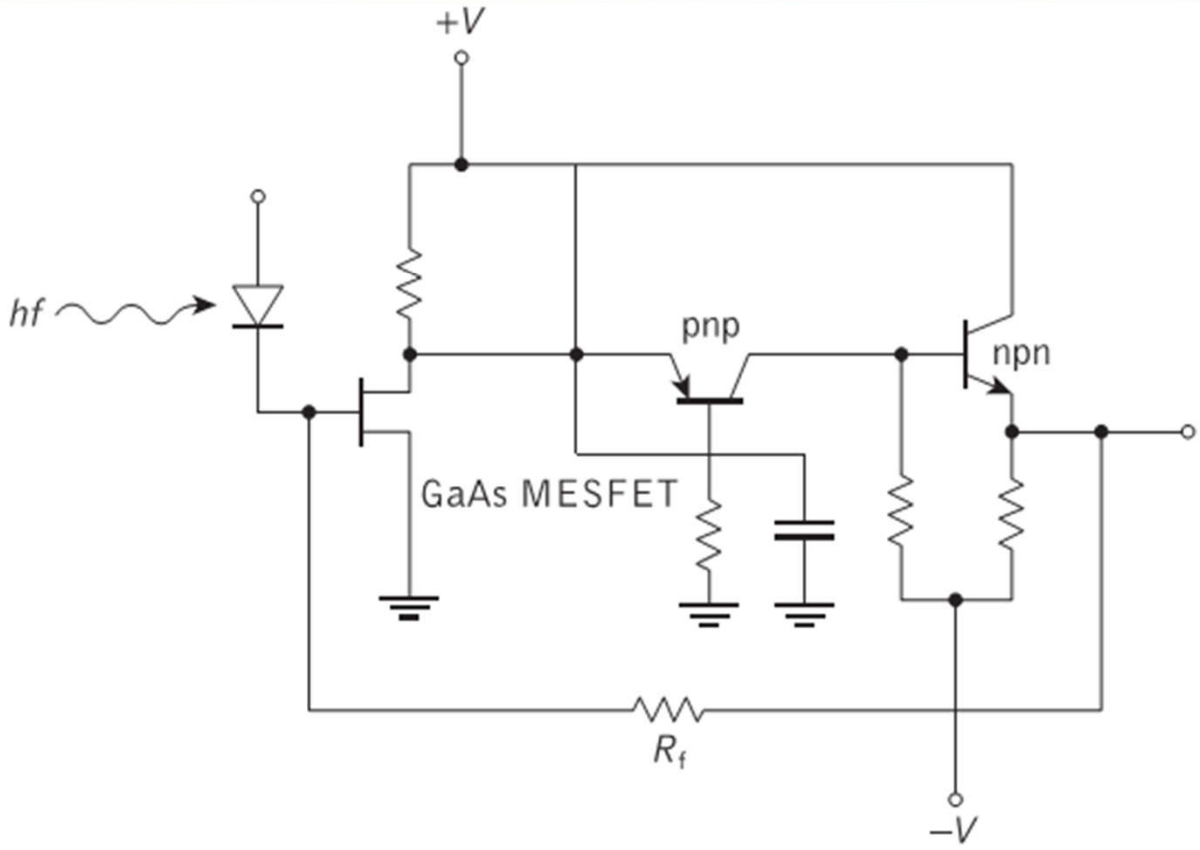


**Figure 9.14** PIN–FET hybrid transimpedance front-end receiver [Ref. 29]

## 9.6 High-performance receivers

It is clear from the discussions in Sections 9.3 to 9.5 that noise performance is a major design consideration providing a limitation to the sensitivity which may be obtained with a particular receiver structure and component mix. However, two other important receiver performance criteria were also outlined in the aforementioned sections, namely bandwidth and dynamic range. Moreover, distinct trade-offs exist between these three performance attributes such that an optimized design for one criterion may display a degradation in relation to one or both of the other criteria. Nevertheless, although high-performance receiver design may seek to provide optimization for one particular attribute, attempts are generally made to minimize the degradations associated with the other performance parameters. In this section we describe further the strategies that have been adopted to produce high-performance receivers for optical fiber communications, together with some of the performance results which have been obtained over the last few years.

As mentioned in Section 9.5.2, low-noise performance combined with potential high-speed operation has been a major pursuit in the hybrid integration of *p–i–n* photodiodes with GaAs MESFETs. In this context it is useful to compare the noise performance of various transistor preamplifiers over a range of bandwidths. A theoretical state-of-the-art performance comparison for the silicon junction FET (JFET), the silicon metal oxide semiconductor FET (MOSFET) and the silicon bipolar transistor preamplifier with a GaAs MESFET device for transmission rates from 1 Mbit $s^{-1}$ to 10 Gbit $s^{-1}$ is shown in Figure 9.15 [Ref. 37]. It may be observed that at low speeds the three FET preamplifiers provide higher sensitivity than the Si bipolar device. In addition it is apparent that below 10 Mbit $s^{-1}$ the Si MOSFET preamplifier provides a lower noise performance than the GaAs MESFET. Above 20 Mbit $s^{-1}$, however, the highest sensitivity is obtained with the GaAs MESFET device, even though at very high speeds the Si MOSFET and Si bipolar transistor preamplifiers exhibit a noise performance that is only slightly worse than the

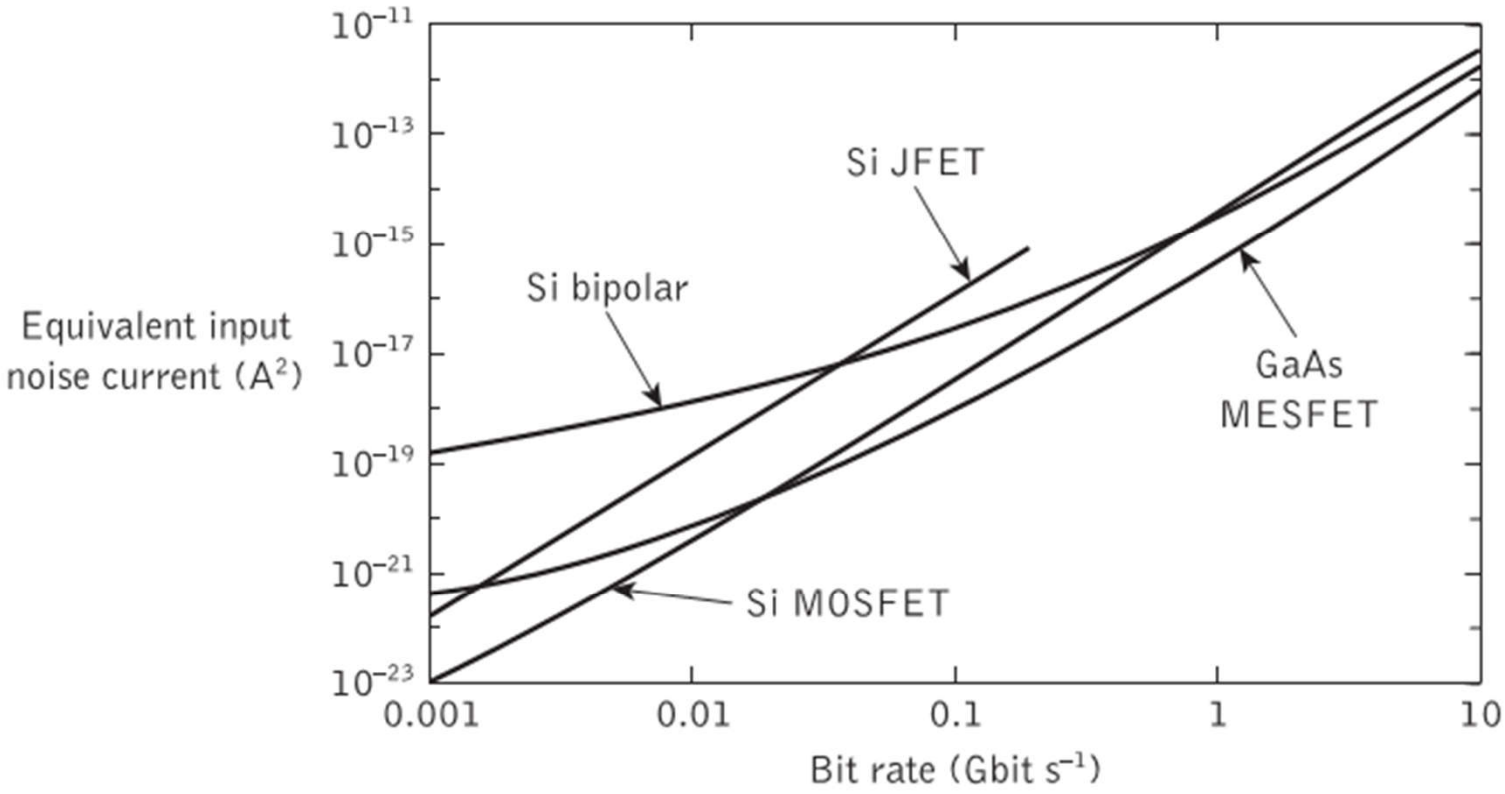


**Figure 9.15** Noise characteristics for various optical receiver transistor preamplifiers. Reproduced with permission from B. L. Kasper, 'Receiver design', in S. E. Miller and I. P. Kaminow (Eds), *Optical Fiber Telecommunications II*, Academic Press Inc., p. 689, 1988, © Elsevier

aforementioned device. Furthermore, it is clear that, as indicated in Section 9.5, the Si bipolar transistor preamplifier displays a noise improvement over the Si JFET, in this case at speeds above 50 Mbit $s^{-1}$.

The optimization of PIN–FET receiver designs for sensitivity and high-speed operation has been investigated [Refs 38, 39]. Also a wideband (10 GHz), low-noise device using discrete commercial components has been reported [Ref. 40]. In addition, new high-speed, low-noise transistor types have been investigated for optical receiver preamplifiers. These devices include the heterojunction bipolar transistor (HBT) [Ref. 41] and high electron mobility transistor (HEMT) [Refs 42, 43]. The latter device type comprises a selectively doped heterojunction FET which has displayed 3 dB bandwidths up to 20 GHz within the three-stage optical preamplifier illustrated in Figure 9.16(a) [Ref. 42]. Each stage comprised a shunt feedback configuration containing a single HEMT with mutual conductance of 70 millisiemens and a gate to source capacitance of 0.36 pF (see Figure 9.16(b)). When operated with an InGaAs *p–i–n* photodiode, the preamplifier exhibited a 21.5 dB gain with an averaged input equivalent noise current density of 7.6 pA $Hz^{-\frac{1}{2}}$ over the range 100 MHz to 18 GHz.

Although the above discussion centered on *p–i–n* receiver preamplifier designs, high-speed APD optical receivers have also been investigated [Refs 44–46]. In particular, a high-sensitivity APD–FET receiver designed to operate at speeds up to 8 Gbit $s^{-1}$ and at wavelengths in the range 1.3 to 1.5 μm is shown in Figure 9.17 [Ref. 45]. The receiver employed a 60 GHz gain–bandwidth product InGaAs/InGaAsP/InP APD followed by a hybrid GaAs MESFET high-impedance front end. Moreover, a receiver sensitivity of –25.8 dBm was obtained for a BER of $10^{-9}$.

An additional strategy for the provision of wideband, low-noise receivers, especially using the *p–i–n* photodiode detector, involves the monolithic integration of this device type with III–V semiconductor alloy FETs or HBTs [Refs 47–51]. Such monolithic integrated receivers or optoelectronic integrated circuits (OEICs) are discussed further in

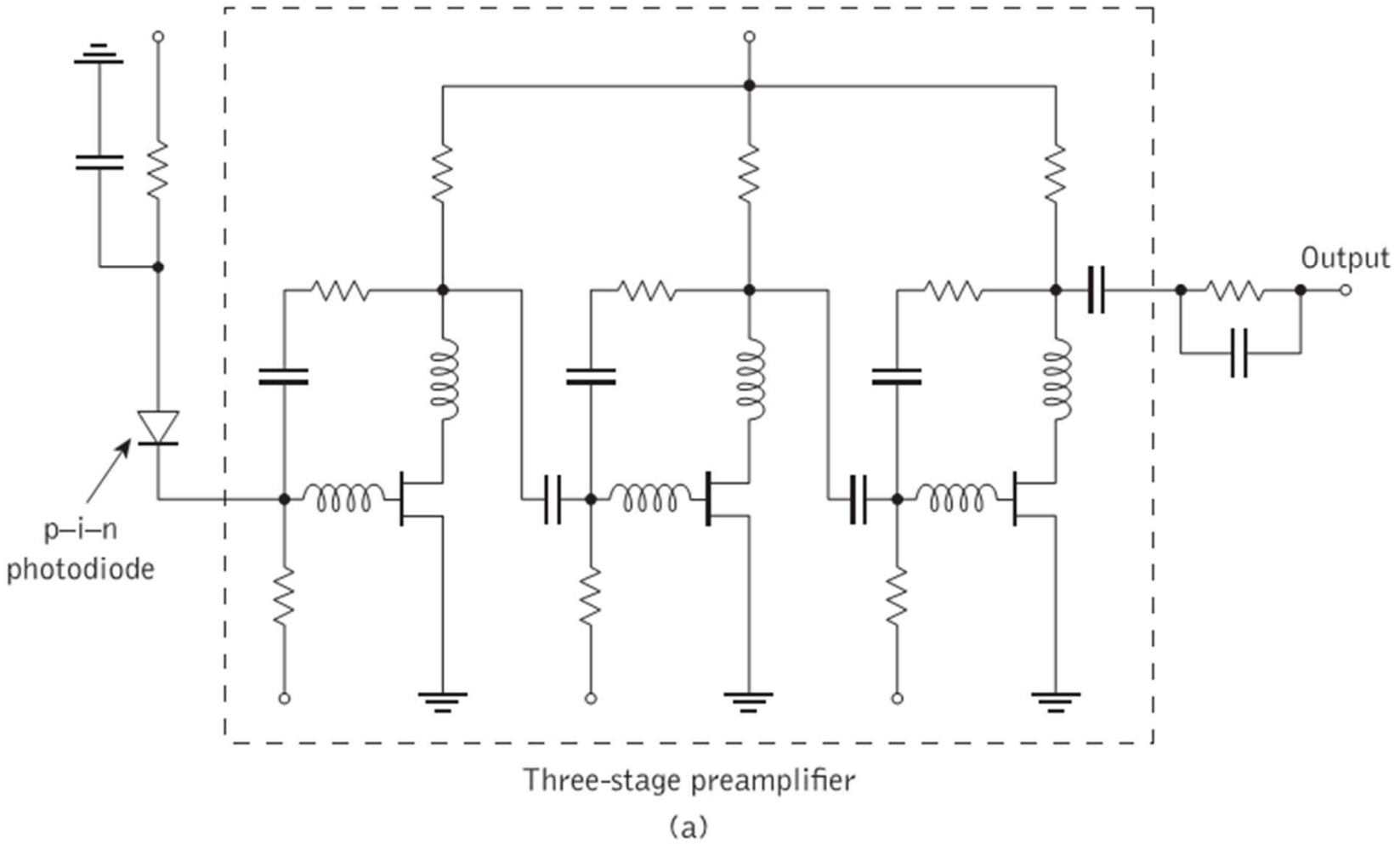


**Figure 9.16** Circuit configuration for a high-speed optical receiver using an HEMT preamplifier [Ref. 42]: (a) *p–i–n*–HEMT optical receiver; (b) single-shunt feedback stage

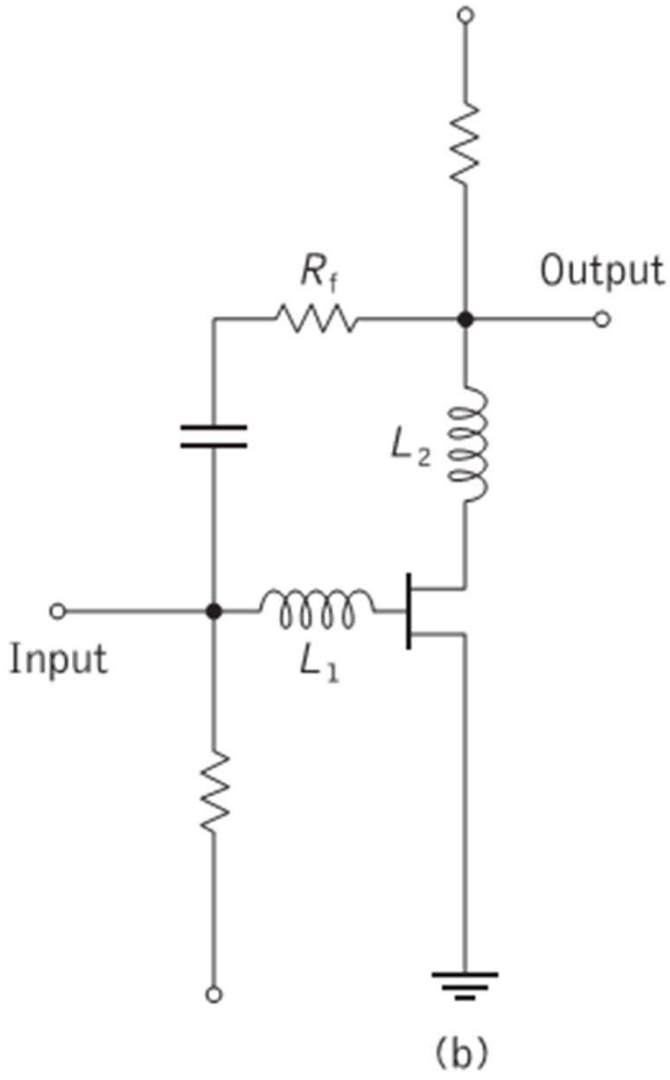


**Figure 9.16** Circuit configuration for a high-speed optical receiver using an HEMT preamplifier [Ref. 42]: (a) *p–i–n*–HEMT optical receiver; (b) single-shunt feedback stage

Chapter 11. However, it should be noted that the major recent activities in this area have concerned devices for operation in the 1.1 to more 1.6 μm wavelength range. An example of the circuit configuration of a monolithic PIN–FET receiver is illustrated in Figure 9.18 [Ref. 51]. The design comprises a voltage variable FET feedback resistor which produces active feedback as an input shunt automatic gain control (AGC) circuit which extends the dynamic range by diverting excess photocurrent away from the input of the basic receiver. Furthermore, the shunt FET gives additional dynamic range extension through

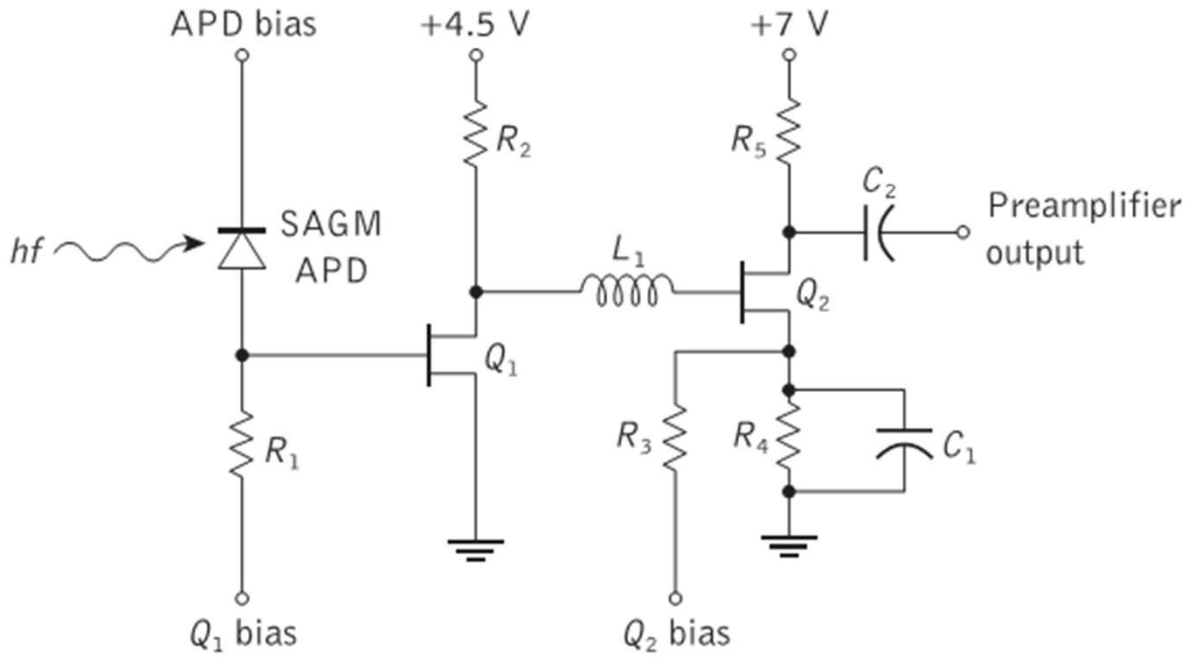


**Figure 9.17** Circuit configuration for a high-sensitivity APD–FET optical receiver [Ref. 45]

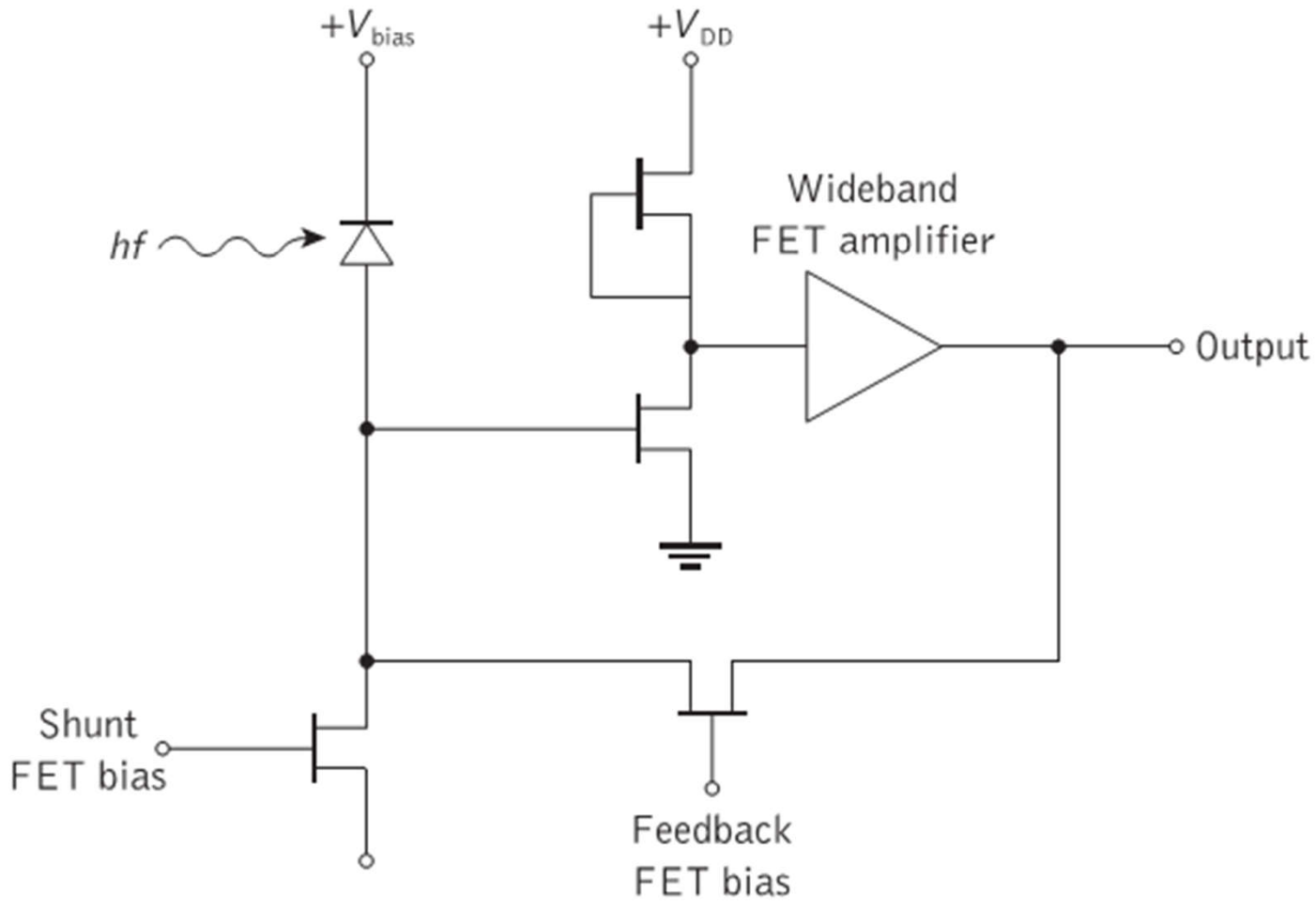


**Figure 9.18** Monolithic PIN–FET optical receiver circuit configuration

the mechanism of active receiver bias compensation, which is discussed further in relation to Figure 9.20 following.

The receiver dynamic range is an important performance parameter as it provides a measure of the difference between the device sensitivity and its saturation or overload level. A receiver saturation or overload level is largely determined by the value of the photodiode bias resistor or, alternatively, the feedback resistor in the transimpedance configuration. Because the photodiode bias resistor has a small value in the low-impedence front-end design, the saturation level is high.* Similarly, the relatively low value of feedback resistor in the transimpedance configuration gives a high saturation level which, combined with a high sensitivity, provides a wide dynamic range, as indicated in Section 9.4.3. By contrast

* Unfortunately, the sensitivity of the low-impedance configuration is poor and hence the dynamic range is generally not large.

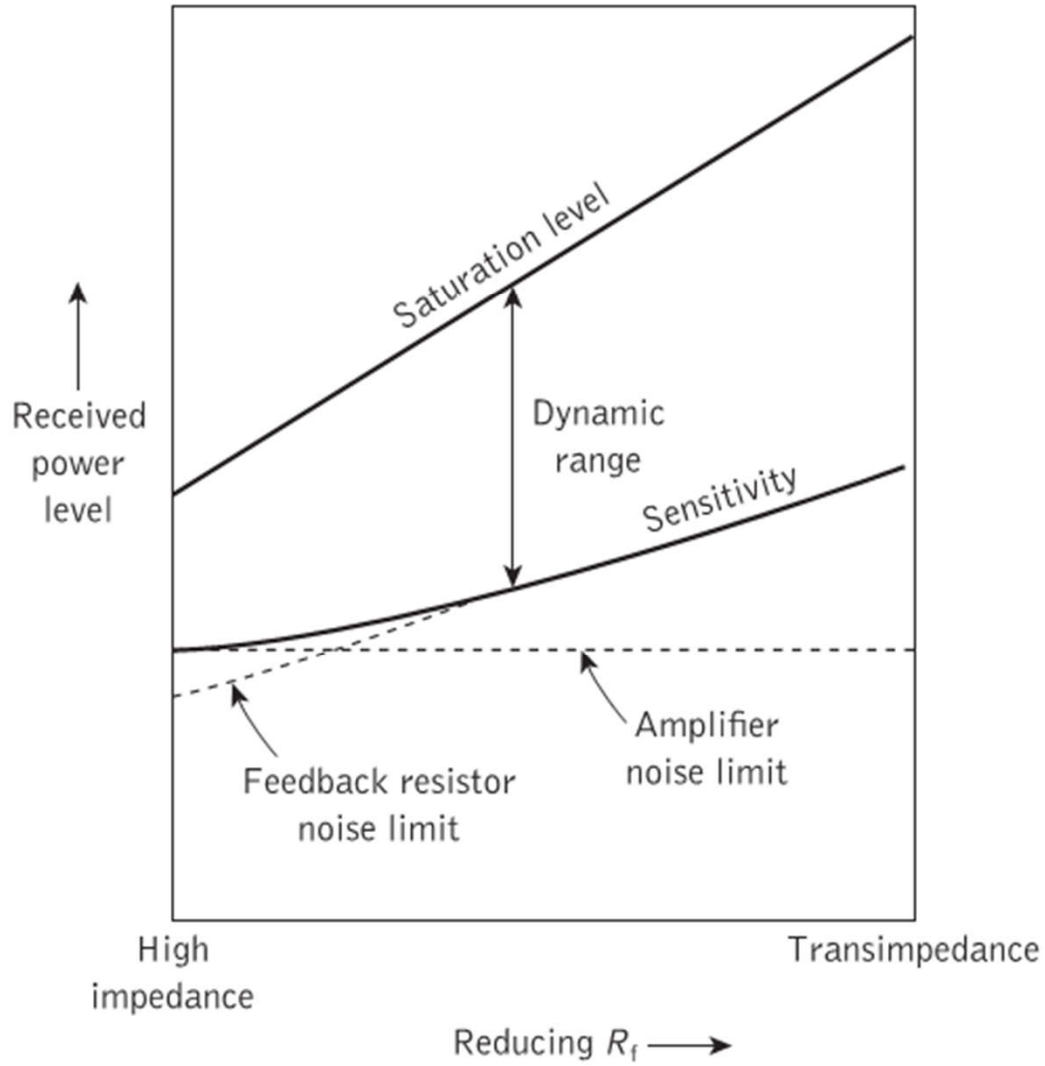


**Figure 9.19** Characteristics illustrating the variation in received power level against the value of the feedback resistor $R_f$ in the transimpedance front-end receiver structure. The high-impedance front-end receiver corresponds to $R_f = \infty$

the high value of photodiode bias resistor in the high-impedance front end causes a low saturation level which, even taking account of the high sensitivity of the configuration, gives a relatively narrow dynamic range. The difference between the two latter receiver structures may be observed in the dynamic range and sensitivity characteristics shown in Figure 9.19. Although the sensitivity decreases in moving from the high-impedance design (left hand side) to the transimpedance configuration (right hand side) as the value of the feedback resistor $R_f$ is reduced, the saturation level increases at a faster rate, producing a significantly wider dynamic range for the transimpedance front-end receiver.

The significance of the receiver dynamic range becomes apparent when the reader considers the ideal multipurpose use of such a device for operation with a variety of optical source powers over different fiber lengths. Moreover, when a high-impedance receiver with a 1 MΩ bias resistor is utilized, the saturation level occurs at an input optical power of 0.5 μW or −33 dBm. Therefore, this device can only be employed in long-haul communication applications where the input power level is low. Corresponding figures for the transimpedance configuration (1 kΩ feedback resistor) and the low-impedance front end (200 Ω bias resistor) are 0.5 mW (−3 dBm) and 2.5 mW (+4 dBm). In all cases the saturation level can be substantially improved by using active receiver bias compensation, as illustrated schematically in Figure 9.20. Hence, as the d.c. voltage at the input to the amplifier increases with the incident optical power, the control loop applies an equal but opposite shift in the voltage to the other side of the bias resistor. In this way the voltage at the input to the preamplifier becomes independent of the detected power level. However, in practice the feedback voltage in the control loop cannot be unbounded and therefore the

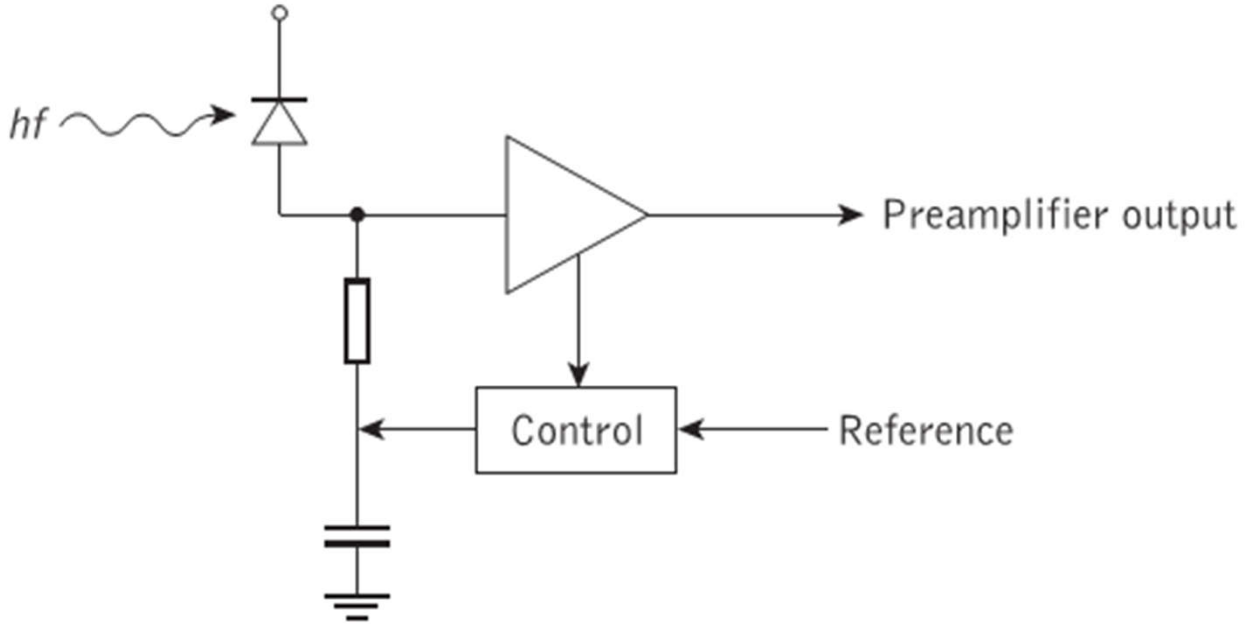


**Figure 9.20** Active receiver bias compensation

technique has limitations. Nevertheless, saturation levels for high-impedance front-end receiver designs may be improved to around 20 μW, or 17 dBm, using this technique.

Even when using bias compensation with a high-impedance front-end receiver to improve the saturation level, the overall dynamic range tends to be poor. For such a receiver operating at a speed of 1 Gbit $s^{-1}$ it is usually in the range 20 to 27 dB, whereas for a corresponding transimpedance receiver configuration without bias compensation, the dynamic range can be 30 to 39 dB.* Furthermore, in the latter case alternative design strategies have proved successful in increasing the receiver dynamic range. In particular the use of optically coupled feedback has demonstrated dynamic ranges of around 40 dB for *p–i–n* receivers operating at modest bit rates [Refs 52, 53].

The optical feedback technique, which is shown schematically in Figure 9.21, eliminates the thermal noise associated with the feedback resistor in the transimpedance front-end design. This strategy proves most useful at low transmission rates because in this case the feedback resistors employed are normally far smaller than the optimum value for low-noise performance so as to maintain the resistor at a practical size (e.g. 1 MΩ). Moreover, large values of feedback resistor limit the dynamic range of the conventional

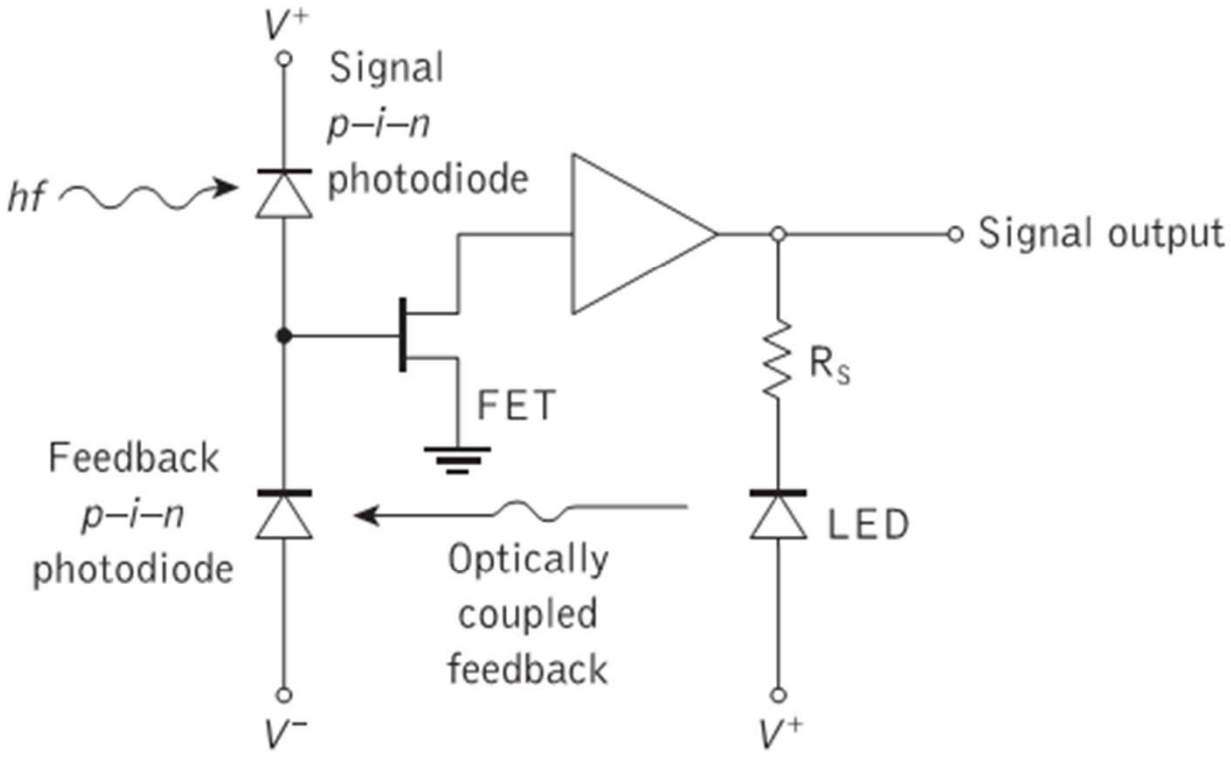


**Figure 9.21** Schematic of optical feedback transimpedence receiver

* It should be noted that in both cases the bottom end of the range refers to *p–i–n* photodiode receivers while the top end of the range is only obtained with APD receivers.

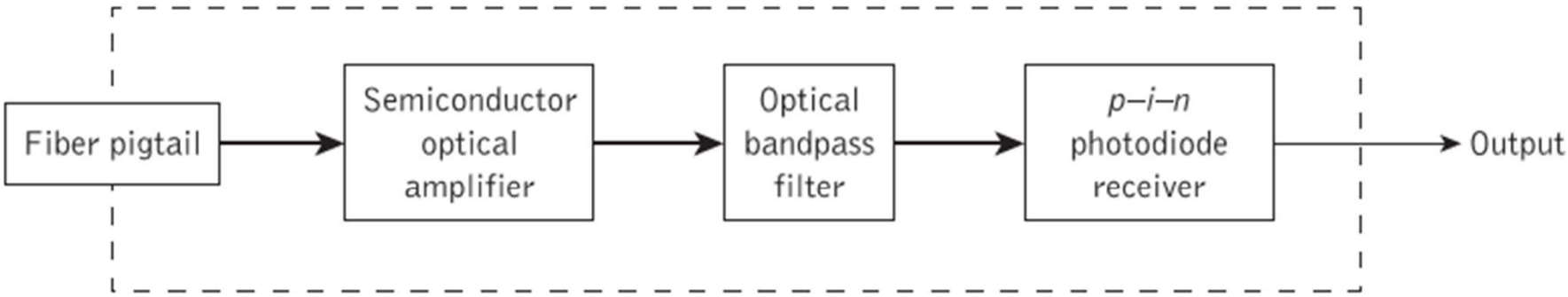


**Figure 9.22** Block schematic of an SOA preamplified *p–i–n* photodiode receiver

transimpedance receiver structure, while also introducing parasitic shunt capacitance which can cause signal integration and hence restrict the bandwidth of the preamplifier. It may be observed from Figure 9.21 that the optical feedback signal is provided by an LED that is driven from the preamplifier output through a small resistor. This resistor acts as a load to generate an output voltage for the following amplifiers. The current feedback to the signal *p–i–n* photodetector is obtained from a second *p–i–n* photodiode which detects the optical feedback signal.

The removal of the feedback resistor in the optical feedback technique allows low-noise performance and hence high receiver sensitivity of the order of –64 dBm at transmission rates of 2 Mbit $s^{-1}$ [Ref. 53]. In addition, as the feedback LED is a low-impedance device that can be driven with a low output voltage, the problem associated with amplifier saturation is much reduced. Therefore this factor, combined with the high sensitivity produced by the strategy, enables wide dynamic range. It should be noted, however, that some penalties occur when employing this technique in that there is an increase in receiver input capacitance and also an increase in detector dark current noise (resulting from the use of two photodiodes) in comparison with the conventional transimpedance preamplifier structure. Nevertheless, it is suggested that the optical feedback receiver component costs can be comparable with resistive feedback designs [Ref. 53] while providing a significant performance improvement.

An alternative strategy for the realization of high-sensitivity receivers, in this case for high-speed operation, is to employ preamplification using an optical amplifier prior to the receiver [Refs 54–58]. The two basic optical amplifier technological types, namely the semiconductor optical amplifier (SOA) and the fiber amplifier, are discussed in Sections 10.3 and 10.4 respectively. It is clear, however, that both device types may be utilized in this preamplification role which is illustrated schematically for an SOA device in Figure 9.22.* The SOA shown in Figure 9.22 operates as a near-traveling-wave amplifier and therefore the output emissions are predominantly spontaneous, creating a spectral bandwidth which is determined by the gain profile of the device. Because the typical spectral bandwidth is in the range 80 to 120 nm, a bandpass optical filter† is employed to reduce the intensity of the spontaneous emission reaching the optical detector. This has the effect of reducing the spontaneous noise products and thus improving the overall receiver sensitivity.

* It should be noted that the corresponding schematic showing a fiber amplifier fulfilling this role is provided in Figure 10.13(c).

† The optimum filter bandwidth is determined by a number of factors including the detector noise, the transmission rate, the transmitter chirp characteristics and the filter insertion loss but is typically in the range 0.5 to 3 nm.

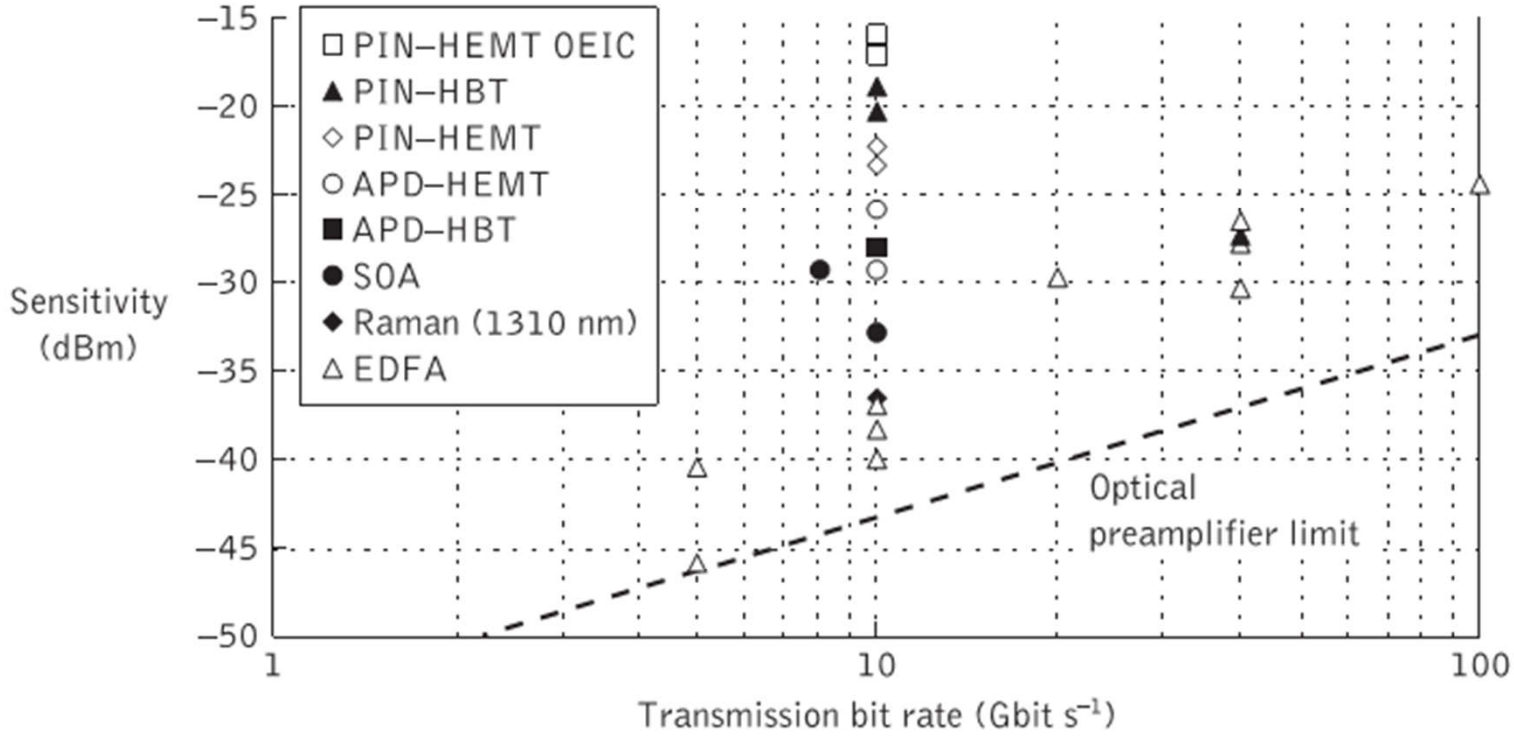


**Figure 9.23** Characteristic showing receiver sensitivity against transmission bit rate for various receiver preamplifier types. Reprinted from Ref. 56 with permission from Elsevier

Although the sensitivity improvement introduced by the laser preamplifier is a function of the device internal gain, the coupling losses between the various elements and the bandwidth of the bandpass filter, it is typically in the range 10 to 15 dB when using an SOA. Moreover, it is interesting to observe from the sensitivity against transmission rate characteristics shown in Figure 9.23 [Ref. 56] that the SOA preamplifier *p–i–n* photodiode configuration illustrated in Figure 9.22 displays a significant improvement over high-performance APD receivers, particularly at speeds of 10 Gbit $s^{-1}$ and above. Figure 9.23 displays the sensitivity provided by different optical receiver preamplifier types in relation to increasing transmission rates up to 100 Gbit $s^{-1}$ [Ref. 56]. It may be observed that the majority of the optical receivers shown operate at transmission rates from 10 to 40 Gbit $s^{-1}$ [Refs 56–59] and that both the SOA and erbium-doped fiber amplifier (EDFA) are useful devices to provide for the optical preamplification. Furthermore, the latter device can attain a receiver sensitivity of –25 dBm with a noise figure value lying between 4 and 5 dB while enabling a high transmission rate of 40 Gbit $s^{-1}$ [Ref. 56]. The SOA, however, exhibits a relatively high noise figure in the range 7 to 8 dB, but its small size, wider operating

wavelength range and potential for monolithic integration make it an important device for optical preamplification (see Section 10.3). For example, an optically preamplified receiver using a vertical cavity SOA (see Section 10.3.3) operating at a signal wavelength of 1.55 μm exhibited a sensitivity of −28.5 dBm at higher transmission bit rates from 10 to 40 Gbit $s^{-1}$. An output signal power penalty of 4.7 dB was observed, however, when receiving the higher bit rates in the region from 20 to 40 Gbit $s^{-1}$ [Ref. 59].

Finally, a germanium on silicon-on-insulator (Ge-on-SOI) technology (see Section 11.2) receiver comprising a *p–i–n* photodiode paired with a high-gain CMOS amplifier has also been shown to operate at a transmission rate up to 15 Gbit $s^{-1}$ with a sensitivity of −7.4 dBm [Re. 60]. Although the demonstrated sensitivity for this receiver was quite modest, it functioned with a single supply voltage of only 2.4 V benefiting from the integration of the Ge-on-SOI *p–i–n* photodiode with the lower power silicon CMOS integrated circuit amplifier.

Although in this chapter we have focused on receiver performance and design techniques for intensity-modulated/direct detection optical fiber communication systems, many of the

strategies discussed are also utilized within the generally more complex receiver structures required to enable coherent transmission. The various coherent demodulation schemes are discussed in some detail in Section 13.6 and the coherent receiver sensitivities are compared both with each other and with direct detection in Section 13.8. However, the specific preamplifier noise and technological considerations are not repeated as they apply equally to both detection techniques.

# Problems

**9.1** Briefly discuss the possible sources of noise in optical fiber receivers. Describe in detail what is meant by quantum noise. Consider this phenomenon with regard to:
(a) digital signaling,
(b) analog transmission,
giving any relevant mathematical formulas.

**9.2** A silicon photodiode has a responsivity of 0.5 A $W^{-1}$ at a wavelength of 0.85 μm. Determine the minimum incident optical power required at the photodiode at this wavelength in order to maintain a bit-error-rate of $10^{-7}$, when utilizing ideal binary signaling at a rate of 35 Mbit $s^{-1}$.

**9.3** An analog optical fiber communication system requires an SNR of 40 dB at the detector with a post-detection bandwidth of 30 MHz. Calculate the minimum optical power required at the detector if it is operating at a wavelength of 0.9 μm with a quantum efficiency of 70%. State any assumptions made.

**9.4** A digital optical fiber link employing ideal binary signaling at a rate of 50 Mbit $s^{-1}$ operates at a wavelength of 1.3 μm. The detector is a germanium photodiode which has a quantum efficiency of 45% at this wavelength. An alarm is activated at the receiver when the bit-error-rate drops below $10^{-5}$. Calculate the theoretical minimum optical power required at the photodiode in order to keep the alarm inactivated. Comment briefly on the reasons why in practice the minimum incident optical power would need to be significantly greater than this value.

**9.5** Discuss the implications of the load resistance on both thermal noise and post-detection bandwidth in optical fiber communication receivers.

**9.6** A silicon *p–i–n* photodiode has a quantum efficiency of 65% at a wavelength of 0.8 μm. Determine:

(a) the mean photocurrent when the detector is illuminated at a wavelength of 0.8 μm with 5 μW of optical power;
(b) the rms quantum noise current in a post-detection bandwidth of 20 MHz;
(c) the SNR in dB, when the mean photocurrent is the signal.

**9.7** The photodiode in Problem 9.6 has a capacitance of 8 pF. Calculate:

(a) the minimum load resistance corresponding to a post-detection bandwidth of 20 MHz;

(b) the rms thermal noise current in the above resistor at a temperature of 25 °C;
(c) the SNR in dB resulting from the illumination in Problem 9.6 when the dark current in the device is 1 nA.

**9.8** The photodiode in Problems 9.6 and 9.7 is used in a receiver where it drives an amplifier with a noise figure of 2 dB and an input capacitance of 7 pF. Determine:
(a) the maximum amplifier input resistance to maintain a post-detection bandwidth of 20 MHz without equalization;
(b) the minimum incident optical power required to give an SNR of 50 dB.

**9.9** A germanium photodiode incorporated into an optical fiber receiver working at a wavelength of 1.55 μm has a dark current of 500 nA at the operating temperature. When the incident optical power at this wavelength is $10^{-6}$ W and the responsivity of the device is 0.6 A $W^{-1}$, shot noise dominates in the receiver. Determine the SNR in dB at the receiver when the post-detection bandwidth is 100 MHz.

**9.10** Discuss the expression for the SNR in an APD receiver given by:

$$\frac{S}{N} = \frac{M^2 I_p^2}{2eB(I_p + I_d)M^{2+x} + \dfrac{4KTBF_n}{R_L}}$$

with regard to the various sources of noise present in the receiver. How may this expression be modified to give the optimum avalanche multiplication factor?

**9.11** A silicon RAPD has a quantum efficiency of 95% at a wavelength of 0.9 μm, an excess avalanche noise factor of $M^{0.3}$ and a capacitance of 2 pF. It may be assumed that the post-detection bandwidth (without equalization) is 25 MHz, and that the dark current in the device is negligible at the operating temperature of 290 K. Determine the minimum incident optical power which can yield an SNR of 23 dB.

**9.12** With the device and conditions given in Problem 9.11, calculate:

(a) the SNR obtained when the avalanche multiplication factor for the RAPD falls to half the optimum value calculated;

(b) the increased optical power necessary to restore the SNR to 23 dB with $M = 0.5M_{op}$.

**9.13** What is meant by the excess avalanche noise factor $F(M)$? Give two possible ways of expressing this factor in analytical terms. Comment briefly on their relative merits.

**9.14** Explain the gain–bandwidth product of an APD receiver in relation to the device multiplication factor. Briefly describe any two APD receivers with high gain–bandwidth products for operation in the longer wavelength (1.3 to 1.6 μm) region.

**9.15** A germanium APD (with $x = 1.0$) operates at a wavelength of 1.35 μm where its responsivity is 0.45 A $W^{-1}$. The dark current is 200 nA at the operating temperature of 250 K and the device capacitance is 3 pF. Determine the maximum possible SNR when the incident optical power is $8 \times 10^{-7}$ W and the post-detection bandwidth without equalization is 560 MHz.

**9.16** The photodiode in Problem 9.15 drives an amplifier with a noise figure of 3 dB and an input capacitance of 3 pF. Determine the new maximum SNR when they are operated under the same conditions.

**9.17** Discuss the three main amplifier configurations currently adopted for optical fiber communications. Comment on their relative merits and drawbacks.

A high-impedance integrating front-end amplifier is used in an optical fiber receiver in parallel with a detector bias resistor of 10 MΩ. The effective input resistance of the amplifier is 6 MΩ and the total capacitance (detector and amplifier) is 2 pF.

It is found that the detector bias resistor may be omitted when a transimpedance front-end amplifier design is used with a 270 kΩ feedback resistor and an open loop gain of 100.

Compare the bandwidth and thermal noise implications of these two cases, assuming an operating temperature of 290 K.

**9.18** A *p–i–n* photodiode operating at a wavelength of 0.83 μm has a quantum efficiency of 50% and a dark current of 0.5 nA at a temperature of 295 K. The device is unbiased but loaded with a current mode amplifier with a 50 kΩ feedback resistor and an open loop gain of 32. The capacitance of the photodiode is 1 pF and the input capacitance of the amplifier is 6 pF.

Determine the incident optical power required to maintain an SNR of 55 dB when the post-detection bandwidth is 10 MHz. Is equalization necessary?

**9.19** A voltage amplifier for an optical fiber receiver is designed with an effective input resistance of 200 Ω which is matched to the detector bias resistor of the same value. Determine:

(a) The maximum bandwidth that may be obtained without equalization if the total capacitance ($C_T$) is 10 pF.

(b) The rms thermal noise current generated in this configuration when it is operating over the bandwidth obtained in (a) and at a temperature of 290 K. The thermal noise generated by the voltage amplifier may be assumed to be from the effective input resistance to the device.

(c) Compare the values calculated in (a) and (b) with those obtained when the voltage amplifier is replaced by a transimpedance amplifier with a 10 kΩ feedback resistor and an open loop gain of 50. It may be assumed that the feedback resistor is also used to bias the detector, and the total capacitance remains 10 pF.

**9.20** What is a PIN–FET hybrid receiver? Discuss in detail its merits and possible drawbacks in comparison with the APD receiver.

**9.21** Identify the characteristics which are of greatest interest in the pursuit of high-performance receivers.

Discuss the major techniques which have been adopted in order to produce such high-performance receivers for use in long-haul optical fiber communications.

## Answers to numerical problems

**9.2** –70.4 dBm
**9.3** –37.2 dBm
**9.4** –70.1 dBm
**9.6** (a) 2.01 μA; (b) 3.59 nA; (c) 55.0 dB
**9.7** (a) 994.7 Ω; (b) 18.19 nA; (c) 39.3 dB
**9.8** (a) 1.137 kΩ; (b) 19.58 μW
**9.9** 40.1 dB
**9.11** –50.3 dBm
**9.12** (a) 14.2 dB; (b) –49.6 dBm
**9.15** 23.9 dB
**9.16** 21.9 dB
**9.17** High-impedance front-end: 21.22 kHz, $4.27 \times 10^{-27}$ $A^2$ $Hz^{-1}$; Transimpedance front-end: 29.47 MHz, $5.93 \times 10^{-26}$ $A^2$ $Hz^{-1}$
**9.18** –23.1 dBm, equalization is unnecessary
**9.19** (a) 159.13 MHz; (b) 160 nA; (c) 79.56 MHz, 11.3 nA, noise power 23 dB down